Triazolylidene iridium complexes for highly efficient and versatile transfer hydrogenation of C=O, C=N and C=C bonds, and for acceptorless alcohol oxidation

Zahra Mazloomi,[a,b] René Pretorius,[b] Oscar Pàmies,[a]* Martin Albrecht[b]* and Montserrat Diéguez[a]*

[a] Departament de Química Física i Inorgànica, Universitat Rovira i Virgili, C/ Marcel·lí Domingo, 1, 43007 Tarragona, Spain. Fax: (+34)977559563; Tel: (+34)977558780; email: montserrat.dieguez@urv.cat

[b] Department of Chemistry and Biochemistry, University of Bern, Freiestrasse 3, 3012 Bern, Switzerland. Tel: (+41)316314644; email: martin.albrecht@dcb.unibe.ch

Abstract

A set of iridium(I) and iridium(III) complexes are reported with triazolylidene ligands that contain pendant benzoxazole, thiazole, and methyl ether groups as potentially chelating donor sites. The bonding mode of these groups was identified by NMR spectroscopy and X-ray structure analysis. The complexes were evaluated as catalyst precursors in transfer hydrogenation and in acceptorless alcohol oxidation. High-valent iridium(III) complexes were identified as most active precursors for the oxidative alcohol dehydrogenation, while a low-valent iridium(I) complex with a methyl ether functionality was most active in reductive transfer hydrogenation. This catalyst precursor is highly versatile and efficiently hydrogenates ketones, aldehydes, imines, allylic alcohols, and most notably also unpolarized olefins, a notoriously difficult substrate for transfer hydrogenation. Turnover frequencies up to 260 h^{-1} were recorded for olefin hydrogenation, whereas hydrogen transfer to ketones and aldehydes reached maximum turnover frequencies larger than 2000 h^{-1}. Mechanistic investigations using a combination of isotope labeling experiments, kinetic isotope effect measurements, and Hammett parameter correlations indicate that the turnover-limiting step is hydride transfer from the metal to the substrate in transfer hydrogenation, while in alcohol dehydrogenation, the limiting step is substrate coordination to the metal center.

1. Introduction

Sustainable production is one of the important challenges our society is currently facing, and catalysis is undoubtedly a key enabling technology in this process. Small amounts of catalyst allow large quantities of compounds to be transformed in fewer reaction steps and with less side products than in uncatalyzed approaches. Research towards improved activity and selectivity of a catalytic system is therefore at the core of sustainable processes for the reduction of costs, waste, and time. The performance of catalytic reactions depends, to a large extent, on the appropriate selection of the ligands, which provides an electronically and sterically well-defined scaffold for homogeneous catalysts. Within this context, thousands of homo- and hetero-donor ligands have been developed, mainly P- and N-containing ligands with either C_2- or C_1-symmetry, although only a few of them have a general scope.[1] Among these, bidentate heterodonor ligands (P-N, P-S, P-P', etc) with different and electronically diverging donor sites have made some of the most fundamental contributions to the development of catalysis.[2] Specifically, P-N bidentate ligands containing oxazoline, oxazole, or thiazole *N*-donor sites have played a key role in catalysis.[1c,2] Our group has contributed to this development by furnishing improved generations of modular heterodonor P-X ligand libraries, obtained from readily available and easy to handle starting materials.[3] Among them, P-N ligand libraries containing more than 300 systematic structural variations were synthesized from inexpensive reagents (*e.g.*, carbohydrates) and containing mainly oxazoline, oxazole and thiazole moieties as the nitrogen functionality.[3c-e]

In the last two decades, N-heterocyclic carbenes (NHCs) have emerged as a class of powerful ligands for promoting catalytic activity.[4] Owing to their strong σ donor ability, air stability, and low toxicity, NHCs have initially been considered as practical alternatives to the more commonly used phosphines,[4,5] even though there electronic and steric properties are distinct. Because of these unique features, exploring new classes of NHCs has been an attractive target of organometallic chemistry. 1,2,3-Triazolylidene (trz) ligands are a relevant subclass of NHCs possessing a mesoionic carbene (MIC) structure when 1,3-disubstituted.[6] Work by us[7] and others[8] has demonstrated the great potential of this ligand class in catalysis,[9] which has spurred further development. The triazole framework imparts increased σ-donor properties compared to classical Arduengo-type NHCs and the mesoionic character enhances the ability to stabilize different metal oxidation states. In addition, the ligand precursors are accessible via efficient

and functional-group-tolerant "click" chemistry.[6c,10] These features facilitate the synthesis of donor-functionalized MIC ligands with different steric and electronic properties in the quest to maximize catalytic performance.[6] Despite these prospects, the development of heterodonor-containing trz ligands has predominantly focused on pyridyl units, while other heteroatom donor groups have not been explored extensively.[9e,i,11]

Inspired by the potential of trz-based carbene complexes and the success of oxazole/thiazole containing ligands in homogeneous catalysis, we became interested in combining these two scaffolds in a single bidentate ligand and in exploring its potential in catalysis. Herein, the first examples of mixed oxazole/thiazole-trz ligands **L1**H·OTf and **L2**H·OTf and their iridium(I) and iridium(III) complexes **1**–**4** are reported and compared with analogues **5–7** containing an ether-functionalized trz ligand derived from **L3**H·BF_4[11d] (Figure 1).

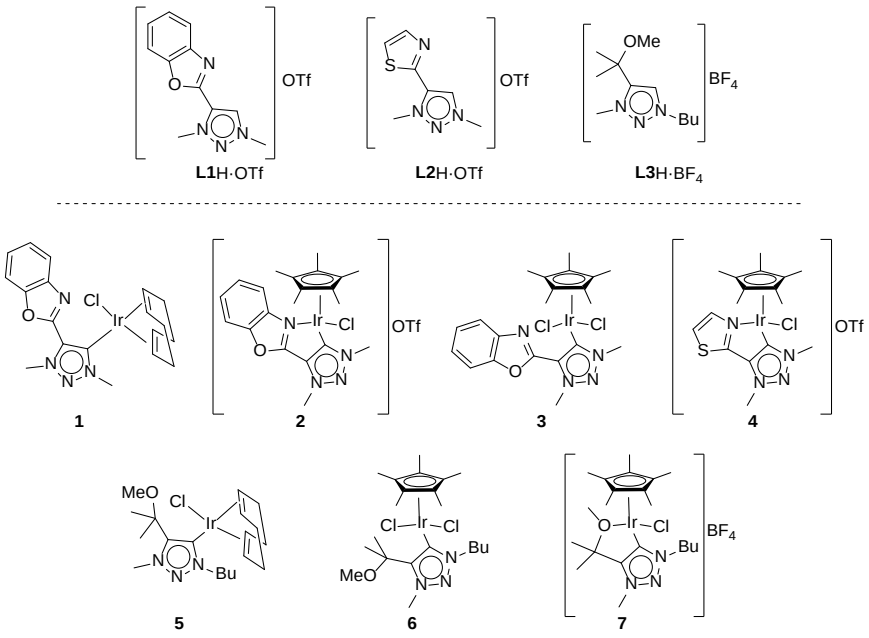

Figure 1. Benzoxazole-, thiazole-, and ether-functionalized triazolylidene ligand precursors **L1**H·OTf, **L2**H·OTf, and **L3**H·BF_4, respectively, and their Ir(I)/Ir(III) complexes **1**–**7** used in this work.

In addition to synthetic and structural aspects, we also present the application of these complexes in transfer hydrogenation catalysis and acceptorless alcohol oxidation. Mechanistic insights were obtained through isotope labeling studies, and correlation of Hammett parameters with reaction rates. Specifically, the most active catalysts are not only active for a broad range

of classic substrates (ketones, aldehydes, imines) but also catalyze the transfer hydrogenation of unpolarized di- and trisubstituted olefins.

2. Results and discussions

2.1. Synthesis and characterization of ligands and complexes

The benzoxazole/thiazole-triazolium salts **L1**H·OTf and **L2**H·OTf used as ligand precursors were prepared via copper-catalyzed [3+2] cycloaddition of methyl azide and the corresponding functionalized trimethylsilyl-protected alkyne, followed by methylation of the triazole at the N3 position (Scheme 1). This procedure yielded the desired benzoxazole-triazolium salt **L1**H·OTf as a sole product when starting from the TMS-protected alkynyl benzoxazole, but gave a mixture of thiazole-triazolium salt (desired ligand **L2**H.OTf) and triazole-thiazolium salt (**10**) when starting from the thiazole-triazole **9** (*ca.* 1:3 ratio). The unselective methylation of the thiazole-triazole **9** is attributed to the similar pKa of the two heterocycles, while the basicity of the benzoxazole in **8** is substantially lower than that of triazole and hence leads to the exclusive formation of **L1**H·OTf. Pure salts **L2**H·OTf and **10** were obtained after separation by column chromatography. The formation of ligand precursors **L1**H·OTf and **L2**H·OTf was confirmed by ^{1}H and ^{13}C NMR spectroscopy and mass spectrometry. For ligand **L1**H·OTf single crystals suitable for X-ray diffraction analysis were obtained and diffraction analysis further confirms its formation (see Supporting Information). The triazolium-ether salt **L3**H·BF_4 was prepared for comparative purposes according to previously reported procedures.[11d]

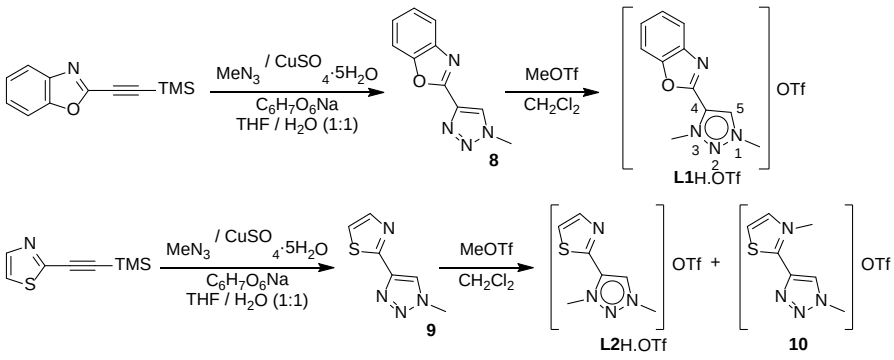

Scheme 1. Synthesis of triazolium-benzoxazole/thiazole salts **L1**H·OTf and **L2**H·OTf.

Iridium complexes **1**–**7** were obtained by a one-pot reaction from the corresponding triazolium salts **L1**–**L3**H·X. Reaction with Ag_2O and Me_4NCl yielded the desired Ag-carbene intermediates, and subsequent in situ transmetalation with either $[Ir(\mu\text{-}Cl)(cod)]_2$ or

$[Ir(Cp^*)Cl_2]_2$ gave complexes **1–7** (Scheme 2). Note that under these reaction conditions, we were unable to prepare the iridium(I) analogue of complex **1** containing a thiazole instead of a benzoxazole donor group. When using the triazolium-benzoxazole salt, metalation with the iridium(III) precursor compound $[IrCl_2(Cp^*)]_2$ produced a 3:1 mixture of complexes **2** and **3** with bidentate and monodentate coordination of the triazolylidene ligand, respectively. Both complexes, **2** and **3**, were obtained in pure form after separation by column chromatography. The Ir(III) complexes **6** and **7** were synthesized as previously described.[11d]

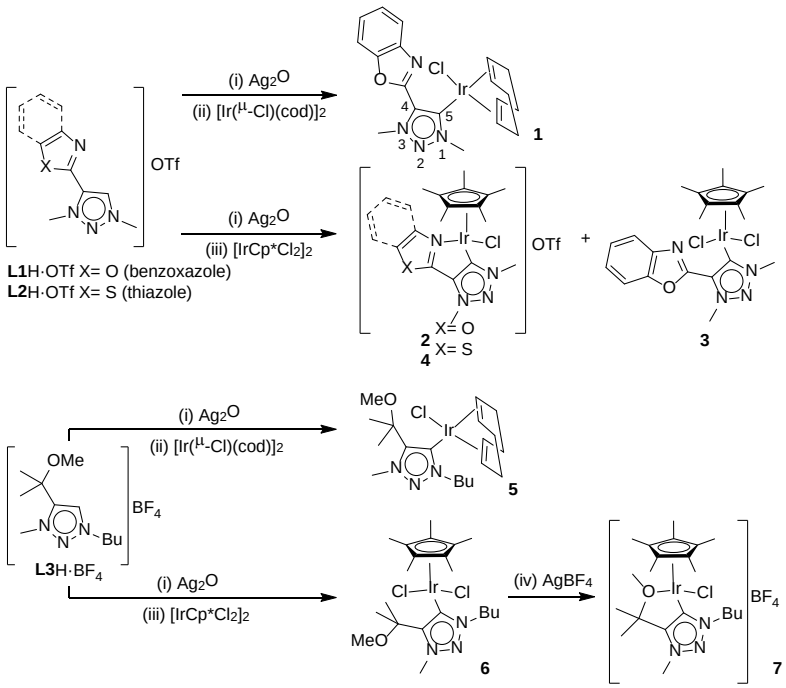

Scheme 2. Synthesis of benzoxazole/thiazole/ether-appended 1,2,3-triazol-5-ylidene iridium complexes **1**–**7**.

All complexes were obtained as air-stable solids and were fully characterized by ^1H and ^{13}C NMR spectroscopy, elemental analysis, mass spectrometry and X-ray diffraction. Metal coordination of the 1,2,3-triazolylidene group was confirmed by the disappearance of the triazolium H-5 proton resonance in the ^1H NMR spectra and by the large downfield shift of the iridium-bound C-5 carbon signal in the ^{13}C NMR spectra (Table 1), which is more pronounced in the iridium(I) complexes than in the iridium(III) analogues. In the [IrCl(**L**)(cod)] complexes **1** and **5**, monodentate ligand coordination through the trz group was also confirmed by the distinct resonance frequency of all four methinic groups of the cyclooctadiene ligand, which are diastereotopic due to (unresolved) planar chirality of the complexes. Two sets of signals at significantly different chemical shifts were observed for the methine protons around $\delta_H = 4.5$

and 2.8 ppm each, characteristic of methinic protons *trans* to chloro and *trans* to carbene ligands, respectively.[12] Likewise, four distinct resonances appeared for the methine carbons (*ca.* 80 ppm and 50 ppm in the ^{13}C NMR spectrum; Table 1).

Table 1. Selected ^{1}H and ^{13}C NMR signals for complexes **1**–**5** and ligands **L1**–**L3**H·X [a]

	^{13}C				^{1}H
Compound	C-5	C-4	O–C=N	CH_{cod}	CH_{cod}
1	176.7	133.3	154.4	83.3; 82.9	4.62 (bs); 4.51 (bs)
				52.1; 51.7	2.88 (bs); 2.8b (bs)
2	161.1	136.4	154.5	-	-
3	152.0	135.5	151.9	-	-
4	158.4	145.7	158.4	-	-
5	169.0	146.7	-	81.3; 79.8	4.55 (m); 4.44 (m)
				51.3; 51.1	2.68-2.82 (m)
L1H·OTf	132.3	132.6	151.2	-	-
L2H·OTf	131.0	136.9	150.3	-	-
L3H·BF_4[11d]	146.9	130.0	-	-	-

[a] Otherwise noted all resonances are singlets unless noted otherwise (bs= broad singlet; m= multiplet).

The ability of ligand **L1** to bind in a mono- or bidentate coordination mode to the iridium(III) center was easily confirmed by ^{13}C NMR spectroscopy. Thus, the signal of the quaternary O-C=N nucleus was shifted downfield to 154.5 ppm when the ligand was coordinated in a bidentate fashion as in complex **2**, while it appeared at 151.9 ppm in complex **3** with a monodentate triazolylidene, similar to the chemical shift of the ligand precursor.

Suitable crystals for X-ray diffraction analysis were obtained for complexes **1–5**.[13] The molecular structures confirm the proposed connectivity patterns and show the expected square-planar and piano-stool arrangements for Ir(I) and Ir(III)-complexes, respectively (Figure 2). Comparison of the different structures reveals interesting details. For example, the Ir(III) complexes **2** and **3** both contain the benzoxazole-triazolylidene ligand **L1**, though a slight contraction of the Ir–C5 and Ir–Cl bonds is noted upon chelation in complex **2**, which can be attributed to the cationic nature of the complex when the ligand is bidentate coordinated (Table 2). The C5–Ir bond is longer in the iridium(I) complex **5** than in the iridium(III) complexes (*cf.* 2.063(4) *vs* 2.035(5) in complexes **1** and **5**). Bidentate coordination of **L1** is also responsible for the smaller Ir–C5–C4 angle in complex **2** compared to **3**. This distortion is compensated by

the increase of the Ir–C5–N1 angle, producing yaw angles[14] of 11.6(2)° in both complexes (Table 2). These yaw angles are smaller than those in related pyridyl-trz bidentate complexes.[15] The two chelate structures **2** and **4** have very similar bond metrics about the iridium center, and despite the different heterocyclic ligand (benzoxazole *vs* thiazole), the Ir–N4 bond lengths barely differs in those two complexes. The C5–Ir–N4 bite angles are essentially identical and relatively acute for both complexes (76°, *cf* Table 2) and very similar to those measured for related pyridyl-triazolylidene chelate complexes (76°).[15]

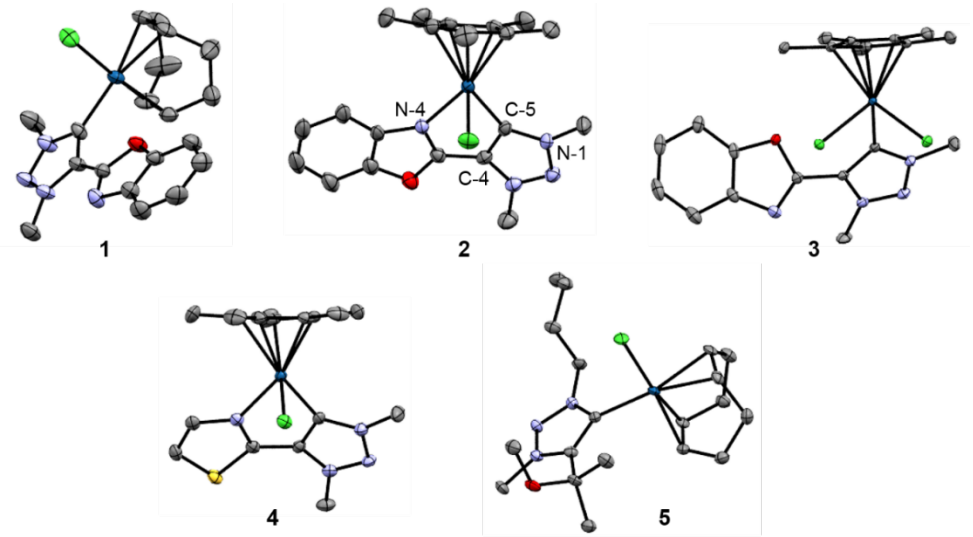

Figure 2. ORTEP plots of the Ir(I) and Ir(III) complexes **1**–**5** (50% probability ellipsoids; H atoms and non-coordinating anions are omitted for clarity).

Table 2. Selected bond distances (Å) and angles (º) for complexes **1**–**5**.

	1	**2**	**3**	**4**	**5**
Ir–Cl	2.3587(16)	2.3949(11)	2.4150(4)	2.4260(9)	2.3635(11)
			2.4205(5)		
Ir–C5	2.035(5)	2.027(4)	2.046(2)	2.022(4)	2.063(4)
Ir–N4	-	2.159(4)	-	2.141(3)	-
C5–C4	1.399(8)	1.380(6)	1.401(3)	1.387(5)	1.396(6)
C5–Ir–N4	-	76.07(16)	-	75.56(13)	-
Cl–Ir–N4	-	86.38(11)	-	90.35(8)	-
C5–Ir–Cl	91.8 (2)	84.97(13)	87.87(5)	88.69(10)	91.39(12)
			88.06(6)		
Ir–C5–C4	132.9(4)	117.8(3)	131.76(14)	117.2(3)	135.7(3)
Ir–C5–N1	126.1(4)	140.9(4)	126.92(14)	140.5(3)	121.3(3)

2.2. Ir-catalyzed transfer hydrogenation reactions

Catalytic transfer hydrogenation (TH) of unsaturated bonds is currently one of the most investigated hydrogenation reactions. It is a sustainable, efficient and mild method that is operationally simpler and significantly safer than direct hydrogenation which uses molecular hydrogen.[16] Ru-, Rh- and Ir-catalysts bearing NHC ligands have been widely used for TH,[17] with results comparable to Noyori-type catalysts for some substrates. For other substrates, such as heteroaromatic ketones, imines and alkenes, selectivity and turnover frequencies are not optimal yet for TH to be competitive with conventional hydrogenation. For these reasons, efforts are directed towards extending the range of applicable substrates through improved ligand design. So far, only few triazolylidene-type MIC complexes have been reported for transfer hydrogenation, and their substrate scope is generally rather narrow.[9i,11c,18] In addition, most procedures involve substantial amounts of base (typically 10 mol%).[19] The development of catalytic systems that require the least possible amount of base is of great importance because the base is able to promote the metal-free reduction of the substrates[20], and it is corrosive, which hampers the industrial implementation of this methodology.

2.2.1. Screening of catalyst precursors

In a first set of experiments the catalytic properties of the Ir(I) and Ir(III) complexes **1**–**7** were evaluated in the transfer hydrogenation of benzophenone **S1** as model substrate, using 2-propanol as both hydrogen donor and solvent, and NaO^{i}Pr as a base and activator. Time-conversion profiles indicate that all complexes are active immediately and without an observable induction period (Supporting Information SI-3). The results are summarized in Table 3 and indicate that activity is highly dependent on the nature of the catalyst precursor. Thus, Ir(I) precursors **1** and **5** provided much higher activity than Ir(III) analogues **2**–**4** and **6**–**7**, respectively (*i.e*. entry 1 *vs* 2–4; and entry 5 *vs* 6 and 7). A plausible explanation is that the higher electron density at the low-valent metal center facilitates the formation of the metal-hydride species. Generally, complexes **5**–**7** containing the ether-functionalized triazolylidene ligand **L3** induce higher activity than complexes **1**–**4** with benzoxazole or thiazole donor groups.[21] This difference was tentatively attributed to the higher propensity of the benzoxazole and thiazole moieties to coordinate to iridium compared to the methyl ether unit in **L3**.[22] It should be noted that the activity profiles and turnover frequencies of complexes **2** and **3** with the benzoxazole as (potentially) chelating group differ substantially, suggesting that the catalytically active species are different and depend on whether the initial species contains a chelating triazolylidene ligand or not.

Further optimization of base and catalyst loading was performed with complex **5**, which exhibited the highest activity under the initial reaction conditions.[23] The amount of base had a substantial impact on activity (Table 1, entries 5 and 8–10): lowering the amount of NaO^{i}Pr from 5 to 2.5 mol% decreased the catalytic performance markedly as indicated by a more than 10 fold lower turnover frequency, and by an increase of the reaction times by more than one order of magnitude to reach completion (entry 9 *vs* 5). Increasing the concentration of the base did not improve activity substantially (initial TOF = 780 *vs* 840 h^{-1}, entries 5 and 8), and therefore, 5 mol% NaO^{i}Pr was used in further reactions. The amount of catalyst precursor had little impact on activity, and initial rates were only moderately varying (TOF = 780–1100 h^{-1}), yet time to completion increased with lower catalyst loading (Table 1, entries 5 and 11–13). Evaluation of the TOF *vs* catalyst concentration suggests a linear dependence, indicating that the reaction is first order in catalyst. It is worth noting that TOFs > 1100 h^{-1} with only 0.1 mol% catalyst loading identify complex **5** as one of the most active triazolylidene-based catalysts

known to date,[18] though these TOF are about 2 orders of magnitude lower than the fastest transfer hydrogenation catalysts reported.[24]

Table 3. Transfer hydrogenation of benzophenone **S1** using complexes **1–7**[a]

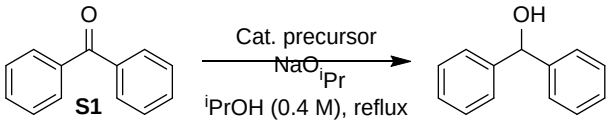

Entry	Cat (mol%)	NaO^{i}Pr /mol%	TOF /h^{-1} [b]	Yield /%[c] (min)
1	**1** (1)	5	250	84 (60)
2	**2** (1)	5	12	8 (60)
3	**3** (1)	5	24	29 (60)
4	**4** (1)	5	60	58 (60)
5	**5** (1)	5	780	97 (30)
6	**6** (1)	5	96	62 (60)
7	**7** (1)	5	72	54 (60)
8	**5** (1)	10	840	97 (30)
9	**5** (1)	2.5	48	97 (400)
10	**5** (1)	1	24	96 (720)
11	**5** (0.5)	5	990	96 (30)
12	**5** (0.25)	5	820	85 (60)
13	**5** (0.1)	5	1100	98 (150)

[a] Reaction conditions: 0.4 M benzophenone **S1** in 2-propanol, catalyst precursor (0.1-1 mol%), NaO^{i}Pr (1-10 mol%). [b] TOF in mol **S1** x (mol cat x h)$^{-1}$ measured after 5 min. [c] Yield measured by ^{1}H NMR spectroscopy using mesitylene as internal standard (in parentheses time required to reach the indicated yield).

2.2.2. Scope and limitations of transfer hydrogenation with complex 5.

Encouraged by these initial results, we investigated complex **5** in the reduction of a broad range of substrates bearing other unsaturated groups such as ketones (**S1**–**S17**), aldehydes (**S18**–**S25**), imines (**S26**, **S27**), α,β-unsaturates ketones (**S28**–**S30**), and allylic alcohols (**S31**, **S32**), and even olefins (**S33**–**S44**). In all cases, the reactions were performed using 0.5 mol% of catalyst precursor **5** and 5 mol% of base.

We first investigated the reduction of 17 ketones with different steric and electronic properties including challenging heteroaromatic ketones (**S1**–**S17**; entries 1–17 Table 4). The results

indicate that the catalytic activity depends on both the steric and electronic properties of the substrate, with TOFs as high as 2100 h^{-1} for the reduction of less sterically demanding cyclohexenone **S2** and electron-poor 4-(trifluoromethyl)acetophenone **S8** (entries 2 and 8). The activity towards reduction of aryl ketones decreased with increasing steric demand of the alkyl substituents (**S1**, **S3**–**S5**, *cf.* entry 5 *vs* 3). However, catalytic activity was hardly affected by steric factors on the aryl moiety of the substrate. Interestingly, *ortho*-substituted aryl ketones were slightly more reactive than the non-substituted analogues (entry 3 *vs* 11). When comparing several *para*-substituted aryl ketones (**S3**, **S6**–**S8**), we note that the catalytic activity increases with enhanced electronic withdrawing character of the *para* substituent (entries 6–8; see also section 2.2.3 for a mechanistic discussion). Finally, the transfer hydrogenation of *meta*-substituted aryl ketones (**S9**, **S10**) provided high activities similar to **S3** (Table 4, entry 3 *vs* 9 and 10).

The scope was then extended to heteroaromatic ketones, which are more challenging substrates because coordination of the heteroatom to the metal often reduces the activity of the catalyst drastically. Therefore, catalytic systems able to reduce this substrate class under transfer hydrogenation conditions are relatively rare.[25] To the best of our knowledge only one study has reported the reduction of 2-acetylpyridine using a cationic Rh(III) complex containing a bis(trz) ligand.[26] When using complex **5**, all evaluated heteroaromatic ketones (**S12**–**S17**, Table 4, entries 12–17) were reduced with very high conversion and TOFs up to 1400 h^{-1}. The activity was strongly dependent on the type of heteroaromatic moiety and on its substitution pattern. For example, furyl-based ketones (**S16** and **S17**) induced slightly higher activities (TOFs up to 1500 h^{-1}) than the phenyl-derived substrates (entries 16, 17 *vs* 3). They also induced higher activities than the pyridyl-based substrates **S12**-**S14**, which we attribute to the lower ability of the furyl group to coordinate to the metal center. The catalytic activity was lowest towards the thienyl-based ketone **S15** (TOF = 100 h^{-1}; entry 15). The reduction of pyridyl-based ketones (**S12**–**S14**, entries 12–14) showed a marked dependence on the heteroaromatic ring substitution pattern and was most efficient with 3- and 4-acetylpyridines (**S12** and **S13**) yet significantly slower for 2-acetylpyridine **S14** (TOF = 260 h^{-1}). Such a trend is not unexpected when considering that both the substrate and the product of 2-acetylpyridine reduction are potentially chelating ligands that may deactivate the catalyst through competitive coordination to the active site. Such an interaction is obviously more effective for **S14** than in the substrates containing the acyl substituent in *meta* or *para* position.

Table 4. Transfer hydrogenation of ketones, aldehydes and imines using Ir-complex **5**[a]

Entry	Substrate	TOF /h^{-1} [b]	Yield /% (min)[c]	Entry	Substrate	TOF /h^{-1} [b]	Yield /% (min)[c]
1	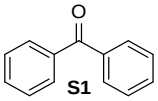 **S1**	990	96 (30)	15	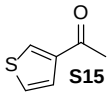 **S15**	100	84 (240)
2	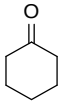 **S2**	1800	97 (5)	16	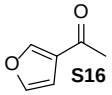 **S16**	1500	96 (30)
3	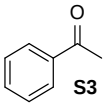 **S3**	1200	98 (30)	17	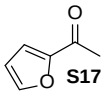 **S17**	1400	93 (30)
4	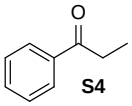 **S4**	1300	96 (15)	18	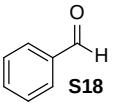 **S18**	1900	98 (10)
5	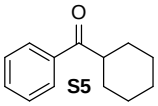 **S5**	500	89 (60)	19	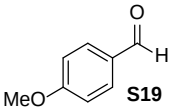 **S19**	1400	97 (15)
6	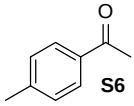 **S6**	1300	99 (30)	20	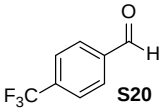 **S20**	2300	99 (5)
7	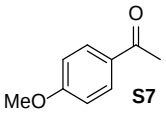 **S7**	770	88 (30)	21	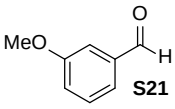 **S21**	1500	96 (15)
8	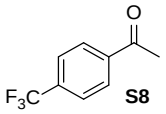 **S8**	2100	98 (5)	22	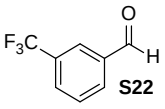 **S22**	1600	94 (15)
9	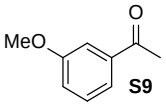 **S9**	1300	96 (30)	23	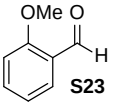 **S23**	1200	98 (30)
10	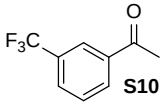 **S10**	1200	95 (30)	24	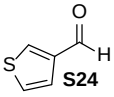 **S24**	150	64 (180)
11	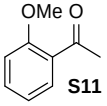 **S11**	1400	98 (30)	25	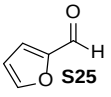 **S25**	1400	91 (30)
12	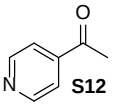 **S12**	510	92 (60)	26	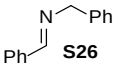 **S26**	770	99 (30)
13	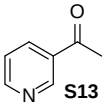 **S13**	480	81 (60)	27	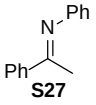 **S27**	30	>99 (24)
14	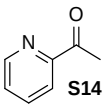 **S14**	260	99 (180)				

[a] Reaction conditions: 0.4 M substrate in 2-propanol, **5** (0.5 mol%), NaO^iPr (5 mol%), reflux. [b] TOF in mol substrate x (mol **5** x h)$^{-1}$ measured after 5 min. [c] Yield measured by ^1H NMR spectroscopy using mesitylene as internal standard or by GC using dodecane as internal standard.

Complex **5** is also a highly efficient catalyst precursor for the TH of several aldehydes (Table 4, entries 18–25). In general complex **5** converts aldehydes significantly faster than ketones and TOFs are 50–100% higher when comparing substrates with identical substitution patterns. The activity follows the same trend as observed for the reduction of ketones, albeit electronic effects are less pronounced. The efficient conversion of aldehydes is remarkable, as commercial grade aldehydes have been used here, which tend to undergo Cannizzarro reactions with many other TH catalysts.[27] No such products from partial oxidation were detected when using complex **5** as catalyst precursor.

The high activity of this complex prompted us to evaluate its activity for the transfer hydrogenation of less reactive substrates. For example, imines are known to be a challenging class of substrates as imine coordination to the catalyst is often too stable, and therefore, higher catalyst loading and much longer reaction times are usually required for efficient conversion. Interestingly, the transfer hydrogenation of aldimine **S26** proceeded smoothly under our mild reaction conditions, reaching a TOF of 770 h^{-1} (entry 26). Ketimine **S27** was also converted, though with a significantly lower TOF (30 h^{-1}), which may be rationalized by the steric demand of this substrate (*cf* faster conversion of aldehyde *vs* ketone, see above). It should be noted that for both substrates, the reduction proceeded cleanly and provided the desired amines as the exclusive products according to ^{1}H NMR spectroscopy.

Hence, catalyst precursor **5** is able to reduce a wide range of ketones, including the most challenging heteroaromatic ones, aldehydes and aldimines with high activities (TOFs up to 2100 h^{-1}). Although there are some metal-carbene species, mainly Ru-NHC complexes that are able to promote these transformations more efficiently,[24d,28] our results compete favorably with known trz iridium catalytic systems.[9i,11c,18a,c,d,f]

In addition to imine hydrogenation, complex **5** was also evaluated in the reduction of α,β-unsaturated ketones and allylic alcohols (Table 5). Full reduction to the corresponding saturated alcohols was observed within 1 hour.

Table 5. Reduction of α,β-unsaturated ketones and allylic alcohols using Ir-complex **5** under transfer hydrogenation conditions[a]

Entry	Substrate	Product	Yield /% (min)[b]
1	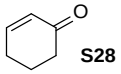 **S28**	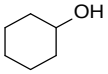	96 (15)
2	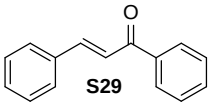 **S29**	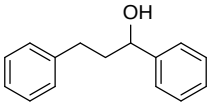	94 (60)
3	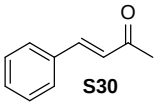 **S30**	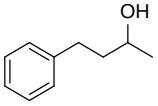	96 (60)
4	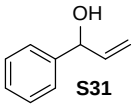 **S31**	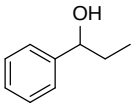	92 (60)
5	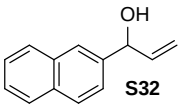 **S32**	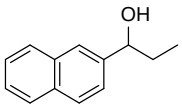	96 (60)

[a] Reaction conditions: 0.4 M substrate in 2-propanol, **5** (0.5 mol%), NaO^{i}Pr (5 mol%), reflux. [b] Yield measured by ^{1}H NMR spectroscopy using mesitylene as internal standard or by GC using dodecane as internal standard.

The high activity of complex **5** towards substrates **S28**–**S32** compares well with the activity towards simple ketones, suggesting that the reaction proceeds via a tandem isomerization/transfer hydrogenation reaction rather than via the direct reduction of the ketone and the olefin as observed by Elsevier et al. using similar Ir(I) complexes containing chelating 1,2,3-triazolylidene-NHC ligands.[18d] To support this mechanistic model, we performed the transfer deuterogenation of α-vinylbenzyl alcohol **S31** using 2-propanol-d_8 as a deuterium source and sodium isopropoxide-d_7 as base (Scheme 3). The formed product contained deuterium not only at the expected position from double bond deuterogenation, but also at the allylic position which corroborates a competing isomerization pathway.[29] A rapid isomerization was also supported by mass spectrometric analysis of the corresponding deuterated products, which revealed species with more than two deuterium atoms incorporated.

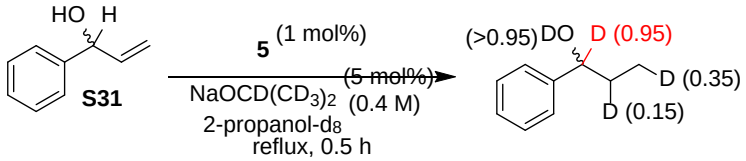

Scheme 3. Deuterium labeling experiments of allylic alcohol **S31** using Ir-catalyst precursor **5**. The percentage of incorporation of deuterium atoms is shown in brackets. Deuterium incorporation due to isomerization shown in red.

Based on the successful conversion of enones and other challenging substrates, we expanded the substrate scope to the transfer hydrogenation of olefins. Olefins are challenging targets because they lack the polarity of ketones and other C=E double bonds and therefore are usually poorly converted in TH. So far only a few catalytic systems containing NHC or MIC ligands have been reported for olefin transfer hydrogenation, and the substrate scope is typically very limited.[11c,17a,10d,18d,30] Previous work by us[17a] and others[17d] suggests that NHC iridium and ruthenium complexes efficiently transfer hydrogenate a small selection of olefins. More recently the groups of Elsevier[18d] and Sarkar[11c] have shown the reduction of cyclooctene using NHC iridium and MIC ruthenium and iridium complexes. However, long reaction times were required (20 h for 50% conversion for the NHC system, 24 h for complete conversion with the MIC ruthenium system), as well as significant catalyst loading (1 mol%) and base (up to 20 mol%). Complex **5**, in contrast, induces the efficient transfer hydrogenation of a broad range of olefins under milder reaction conditions (4-6 h for essentially quantitative conversion at 0.5 mol% iridium and 5 mol% base; Table 6). We note that the catalytic performance is relatively insensitive to the olefin substitution pattern and to the geometry of the double bond, and activities are similarly high for a range of linear mono- and disubstituted olefins, including *E*- as well as cyclic *Z*-olefins with TOFs up to 260 h^{-1} (entries 1–11). Generally, aryl substituents increase the rate compared to alkyl substituents (*cf* entries 3 *vs* 5, or 4 *vs* 7). We also found that the steric effects influence the turnover frequency considerably. For example, transfer hydrogenation of 1,1-disubstituted olefins **S41**–**S43** proceeds at gradually lower rates upon increasing the steric demand of the alkyl substituent (entries 9-11). Similarly, the reduction of sterically even more hindered trisubstituted olefin **S44** was accomplished with the lowest activity of the series and required 12 h to reach synthetically useful conversions. However, it is noteworthy that final conversions are high, and that complex **5** is one of the rare catalyst precursors that is capable of efficiently reducing such a broad range of unpolarized and highly substituted olefins.

Table 6. Transfer hydrogenation of olefins using Ir-complex **5**[a]

Entry	Substrate	TOF /h^{-1} [b]	Yield /% (h)[c]	Entry	Substrate	TOF /h^{-1} [b]	Yield /% (h)[c]
1	 **S33**	170	88 (4)	7	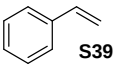 **S39**	190	91 (4)
2	 **S34**	130	93 (6)	8	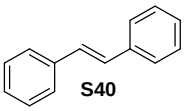 **S40**	240	94 (4)
3	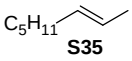 **S35**	170	95 (6)	9	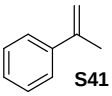 **S41**	200	97 (4)
4	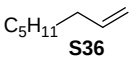 **S36**	160	94 (6)	10	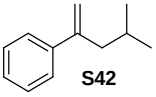 **S42**	190	90 (4)
5	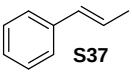 **S37**	260	96 (4)	11	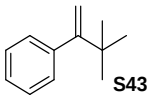 **S43**	110	87 (6)
6	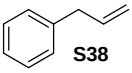 **S38**	260	99 (4)	12	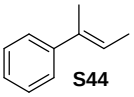 **S44**	80	89 (12)

[a] Reaction conditions: 0.4 M substrate in 2-propanol, **5** (0.5 mol%), NaO^{i}Pr (5 mol%), reflux. [b] TOF in mol substrate x (mol **5** x h)$^{-1}$ measured after 10 min. [c] Yield measured by ^{1}H NMR spectroscopy using mesitylene as internal standard or by GC using dodecane as internal standard.

In an attempt to assess the relative rate of olefin hydrogenation *vs* alkene double bond isomerization, parallel catalytic runs were performed using *trans*-β-methylstyrene **S37** and allylbenzene **S38** as substrates and 2-propanol-d_8 as hydrogen source (Scheme 4). For both substrates, deuterium incorporation took place at the olefinic as well as at the allylic position, and the ratios are equal within measuring errors, which suggests fast isomerization. According to the deuterium incorporation at the terminal position, this isomerization involves an iridium-deuteride species rather than an intramolecular H-transfer. Furthermore, time-dependent GC and ^{1}H NMR analyses indicate that the isomerization is faster than the hydrogenation. Thus, after 10 minutes the allylbenzene **S38** was fully isomerized to the internal olefin **S37** under TH conditions, as indicated by GC analysis (see Supporting Information SI-8).[31] These results confirmed that the reduction of allyl benzene proceeds via a similar tandem isomerization/transfer hydrogenation reaction as discussed for α,β-unsaturated ketones and allylic alcohols (see above).

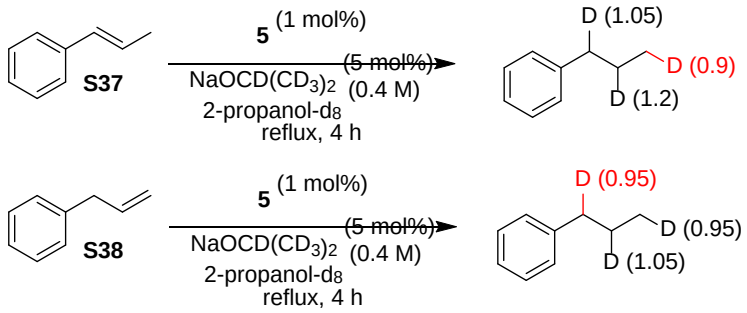

Scheme 4. Deuterium labeling experiments of olefins **S37** and **S38** using Ir-catalyst precursor **5**. The percentage of incorporation of deuterium atoms is shown in brackets. Deuterium incorporation due to isomerization shown in red.

2.2.3. Mechanistic insights

Initial mechanistic investigations of the Ir-catalyzed transfer hydrogenation with complex **5** included the racemization of the mono-deuterated (*S*)-1-phenylethanol-d_1 (*S*)-**12** in the presence of acetophenone **S3** (Scheme 5). This simple experiment has been previously used to elucidate the nature of the metal-hydride species responsible for the catalytic activity.[32] Thus, a selective carbon-to-carbon hydrogen transfer is indicative of a metal-monohydride species responsible for the catalytic activity, while a non-selective hydrogen transfer (involving both oxygen-to-carbon and carbon-to-carbon H-transfer) reveals the involvement of a metal-dihydride species.[16,32] When the reaction was catalyzed with complex **5**, a high degree of retention of deuterium in the α-position (>95%) was observed after full racemization. This result indicates that a monohydride Ir–H species is formed as the catalytically active species, in agreement with previous mechanistic studies on related NHC iridium(I) complexes.[33]

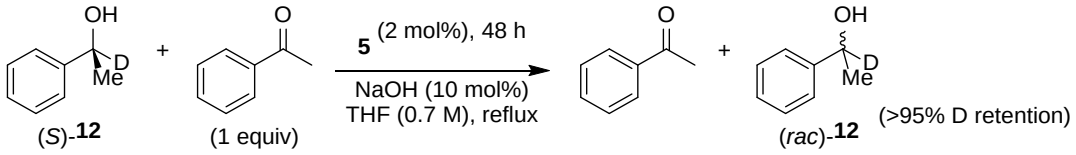

Scheme 5. Deuterium content in 1-phenylethanol-d_1 (*rac*)-**12** after racemization of (*S*)-1-phenylethanol–d_1 using Ir-catalyst precursor **5**.

Further mechanistic insights into the rate determining step of the reaction were obtained by studying the kinetic isotope effects (KIE) of the transfer hydrogenation of acetophenone **S3** and styrene **S39** (Scheme 6). Several experiments were carried out using isopropanol, isopropanol-d_7, and isopropanol-d_8 as solvent, and with sodium *tert*-butoxide instead of sodium isopropoxide as a base to avoid potential base-mediated H/D scrambling. Reaction

monitoring by GC revealed a significant KIE for the hydrogen transfer reaction of both substrates when the carbinol position was deuterated ($k_{CHOH}/k_{CDOH} \approx k_{CHOH}/k_{CDOD} \approx 4$), though the deuteration *vs* protonation of the oxygen did not alter the rate. Likewise, modulation of the solvent from isopropanol-d_7 to isopropanol-d_8 did not affect the rate ($k_{CDOD}/k_{CDOH} \approx 1$).[34] These results clearly indicate that the hydride transfer is the rate-limiting step for both substrate types, while the second process (proton transfer) is comparably fast.

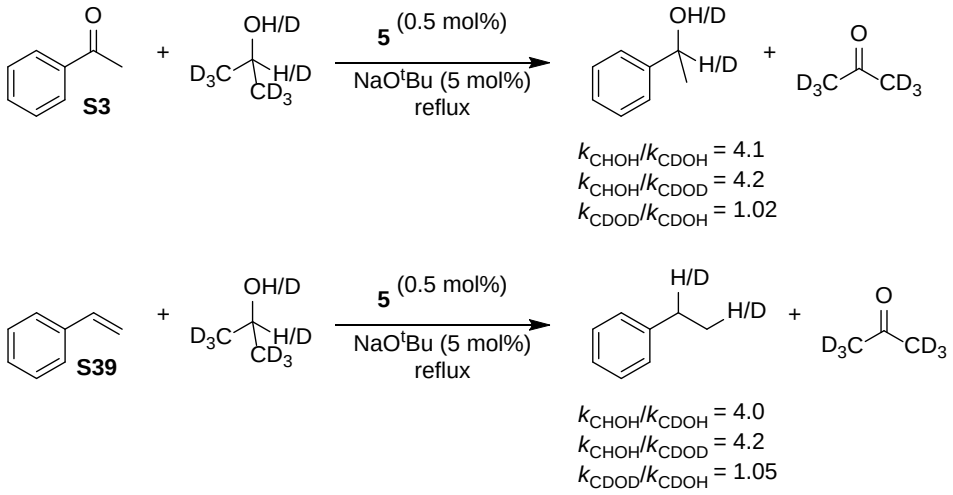

Scheme 6. Kinetic isotope effects of the transfer hydrogenation of ketones (acetophenone **S3** as example) and olefins (styrene **S39** as example) using iridium complex **5**.

To further distinguish whether hydrogen transfer from the isopropanol donor to the metal is turnover limiting or the transfer from the metal-hydride to the substrate, the catalytic conversion of differently *para*-substituted acetophenones (**S3**, **S7**, **S8**) was compared against the Hammett σ values[35] of these substrates (see Figure SI-4 in Supporting Information). The positive ρ value (ρ = 0.52) indicates that the electron density increases in the rate determining step. Combined with the substantial KIE, these results (*i.e.* the fact that the substrate affects the rate as well as the build-up of negative charge according to Hammett parameter correlation) lend strong support to the transfer of the hydride from iridium to the substrate as turnover limiting step

2.3. Ir-catalyzed acceptorless alcohol oxidation

Since transfer hydrogenation inherently involves the dehydrogenation of a donor system such as isopropanol, we were interested to investigate the activity of the iridium complexes **1**–**7** in the dehydrogenation of alcohols. Various procedures are available for the oxidation of

alcohols, ranging from the use of high-valent oxo metal species, Oppenauer-type oxidation and the use of hypervalent iodine among others,[36] to biomimetic and enzymatic approaches using more benign oxidants such as hydrogen peroxide or dioxygen.[37] Acceptorless oxidation of alcohols with liberation of H_2 has been less studied although it is very attractive in terms of atom economy, waste reduction, and reversible hydrogen storage.[38] Research in this area has rapidly moved from phosphine ligands to NHC ligands,[39] including triazolylidene-based catalysts of ruthenium(II) and iridium(III).[9h,j,18,40] One of the drawbacks of oxidant-free dehydrogenation of alcohols is that the product might remain in the coordination sphere and be subsequently transformed into undesired ethers and acetals.[41] Recent work with iridium triazolylidene-based complexes revealed that monometallic species favor the etherification of the carbonyl product, while dimetallic species suppress this transformation and form the ketone selectively.[42]

2.3.1. Dehydrogenation of benzyl alcohol. Catalyst precursor screening

In a first set of experiments, benzyl alcohol **S45** was used as the benchmark substrate to study the effectiveness of the iridium(I) and iridium(III) complexes **1**–**7** in acceptorless alcohol oxidation. For comparison, these complexes were evaluated under the conditions optimized in previous studies of Ir-MIC complexes.[42] Reactions were therefore carried out without base, using a catalyst loading of 5 mol% in 1,2-dichlorobenzene at elevated temperatures (150 °C). Benzaldehyde formation was monitored over time (see Supporting Information) and conversions after 12 and 72 h are compiled in Table 7. For all complexes, the time-conversion profiles showed no significant activation time. Interestingly, only the formation of the desired benzaldehyde was observed in the ^{1}H NMR spectrum, while no etherification was noted.[42] As observed in the transfer hydrogenation reaction, the activity is highly dependent on the catalyst precursor (Table 7). As expected for oxidation reactions and in contrast to reductive TH, high-valent Ir(III) complexes induced much higher activity than the Ir(I) analogues (entry 1 *vs* 2-4; entry 5 *vs* 6-7). Analysis of the catalytic profiles reveals that all systems deactivate, except for complexes **2** and **4** (entries 2 and 4 *vs* 3, 6 and 7). Complex **6** with a pendant ether group shows highest initial activity (TOF_{ini} = 12 h^{-1} compared to TOF_{ini} = 4 h^{-1} for complexes **2** and **4**), though catalytic activity ceased after about 12 h (ca. 60% conversion), while complexes **2** and **4** turn over continuously to full substrate conversion. The enhanced stability of complexes **2** and **4** may be attributed to the stronger coordination of the benzoxazole and thiazole moieties

compared to the methyl ether in complex **6** (*cf* Scheme 2). In contrast to transfer hydrogenation, acceptorless alcohol oxidation benefits from a chelating triazolylidene ligand.

Table 7. Acceptorless oxidation of benzyl alcohol **S45** using complexes **1**–**7**[a]

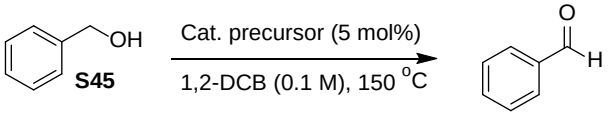

Entry	Cat.	Yield /% (12 h)	Yield /% (72 h)
1	**1**	30	33
2	**2**	33	99
3	**3**	18	34
4	**4**	28	94
5	**5**	30	38
6	**6**	54	60
7	**7**	36	55

[a] Reaction conditions: 0.1 M benzyl alcohol **S45** in 1,2-dichlorobenzene, catalyst precursor (5 mol%). [b] Yield measured by ^{1}H NMR spectroscopy using hexamethylbenzene as internal standard.

2.3.2. Dehydrogenation of other primary and secondary alcohols. Mechanistic insights

Encouraged by the high selectivity induced by the iridium(III) complexes **2** and **4**, their efficiency was assessed with a range of benzylic alcohols **S45**–**S48** and secondary alcohols **S49**–**S52** (Table 8). Generally, conversions were high and good-to-excellent selectivity was achieved. While the substituents of the substrate do not significantly affect the selectivity for secondary alcohols (entries 9–12), a dependence was noted for benzylic alcohols (entries 1–8). Thus, while the electron-poor benzylic alcohol **S47** was converted almost exclusively to the desired aldehyde, methyl groups in *meta* or *para* position (substrates **S46** and **S48**) reduced the selectivity considerably (entry 5 *vs* 3, 7). The formation of the undesired corresponding ethers is lower when using catalyst precursor **4** instead of **2**, suggesting that intrinsic properties of the catalyst structure contribute to controlling the selectivity (entries 4, 8 *vs* 3, 7). The conversion rate is strongly substrate-dependent and is generally higher for secondary than primary alcohols (entries 9–12 *vs* 1–8), and is enhanced by electron-donating groups in the *para* position (*cf* entry 3 *vs* 5, and 10 *vs* 11; see below for mechanistic implications).

Table 8. Base-free dehydrogenation of alcohols using Ir-complexes **2** and **4**[a]

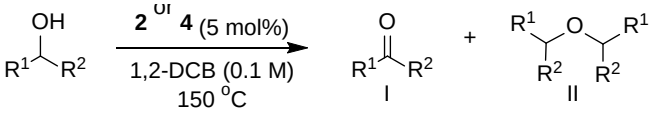

Entry	Substrate	Cat. Precursor	% Yield (h) [b]	I/II Ratio [c]
1	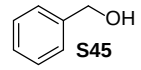 **S45**	**2**	99 (72)	>20/1
2		**4**	94 (72)	>20/1
3	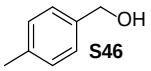 **S46**	**2**	>99 (72)	4/1
4		**4**	99 (72)	10/1
5	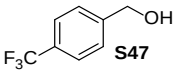 **S47**	**2**	85 (72)	>20/1
6		**4**	64 (72)	>20/1
7	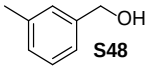 **S48**	**2**	97 (72)	3.3/1
8		**4**	84 (72)	8/1
9	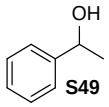 **S49**	**2**	94 (12)	>20/1
10	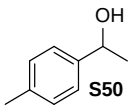 **S50**	**2**	>99 (12)	>20/1
11	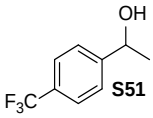 **S51**	**2**	35 (12)	>20/1
12	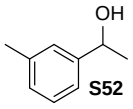 **S52**	**2**	84 (12)	>20/1

[a] Reaction conditions: 0.1 M substrate in 1,2-dichlorobenzene, Ir catalyst precursor (5 mol%). [b] Yield measured by ^{1}H NMR spectroscopy using mesitylene as internal standard or by GC using dodecane as internal standard. [c] Selectivity determined by ^{1}H NMR spectroscopy.

Mechanistic insights were obtained from isotope labeling experiments. Kinetic isotope effects (KIE) of the dehydrogenation reaction were determined by conducting experiments using 1-phenylethanol (CHOH), mono-deuterated 1-phenylethanol-d_1 (CDOH), and bis-deuterated 1-phenylethanol-d_2 (CDOD; Scheme 7). The reactions were monitored over time by GC analysis. In contrast to the transfer hydrogenation reaction, only very small KIEs were obtained ($k_{CHOH}/k_{CDOH} \approx k_{CHOH}/k_{CDOD} \approx 1.1$; $k_{CDOD}/k_{CDOH} \approx 1$). These low values indicate that neither C–H nor O–H bond making or breaking are turnover-limiting processes. Comparison of the activity of complex **2** in the conversion of different *para* substituted benzyl alcohols

(**S45**–**S47**) against their Hammett σ values[35] (see Figure SI-6 in Supporting Information) provides a slope with a negative ρ value (ρ = –0.61), indicating a decrease of electron density in the transition state. A plausible mechanistic model may therefore include the coordination of the substrate alcohol to the iridium center as turnover-limiting step. The substitution of a metal-bound chloride by an alcohol is expected to be faster if the alcohol is electron-rich, which rationalizes the observed Hammett correlation. Such a proposal is in line with a reduced charge density in the substrate upon coordination, and it also concurs with the measured KIEs as no CH or OH bond cleavage is involved. According to this model, solvolysis of the iridium complex and displacement of the Ir–Cl bond by an Ir–O(H)R species is slow and prevents the catalyst from turning over faster. Rate-limiting alcohol coordination also corroborates the observed dependence of the catalytic rate on the ligand structure, as neutral **6** is expected to undergo solvolysis faster than the cationic chelate complexes **2** and **4**. Similar trends were also noted in related alcohol dehydrogenation with triazolylidene ruthenium(II) complexes.[9j]

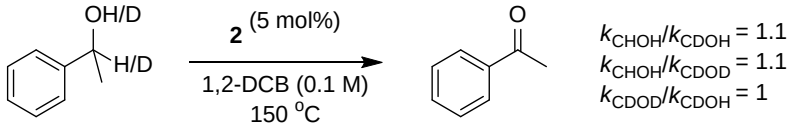

Scheme 7. Kinetic isotope effects of the dehydrogenation of alcohols using Ir-catalyst precursor **2**.

3. Conclusions

We have disclosed efficient and selective hydrogen transfer catalysts that contain a triazolylidene iridium scaffold. Catalytic activity is strongly dependent on the iridium oxidation state and on the donor functionality linked to the triazolylidene ligand. Low-valent iridium(I) complexes perform better in transfer hydrogenation, while high-valent iridium(III) complexes show higher activity for acceptorless alcohol oxidation, especially when the iridium(III) center is stabilized by strongly chelating benzoxazole and thiazole substituents. In contrast, transfer hydrogenation is most efficient when a pendant methyl ether functionality is linked to the triazolylidene ligand, providing excellent activity also to less reactive substrates such as imines and even apolar olefins. These results underline the relevance of ligand tailoring for specific transformations and demonstrate that different ligand design principles are required for transfer hydrogenation catalysis and for alcohol oxidation, including stabilization of low- *vs* high-valent

iridium complexes and weak *vs* strong chelation. Even though it may be intuitive that low-valent complexes show increased activity in reduction (TH), and vice versa, high-valent catalyst precursors in oxidation catalysis, the distinct performance is remarkable as the overall catalytic process is the same hydrogen transfer from/to a substrate. Principally, the microscopic steps of the reaction are therefore expected to be highly related. However, mechanistic investigations reveal completely different rate-limiting steps for the two processes,[43] emphasizing the relevance of sophisticated catalyst design. Moreover, the guidelines deduced from this work may also apply for further optimizing related catalysts for hydrogen transfer reactions.

4. Experimental section

4.1. General considerations. Grubbs columns were used for solvent purification. Anhydrous isopropanol and 1,2-dichlorobenzene were used as commercially available. Compounds 2-((trimethylsilyl)ethynyl)benzo[*d*]oxazole and 2-((trimethylsilyl)ethynyl)thiazole;[44] compound **L3**H·BF_4;[11d] Ir-complexes **6** and **7**;[11d] substrates **S27**,[45] **S31**,[46] **S32**,[46] **S42**,[47] **S43**,[48] **S44**,[49] and (*S*)-1-phenylethan-1-d-1-ol;[32b] and propan-d_7-2-ol[50] were prepared as previously described. All other reagents and substrates were commercially available and used as received. ^{1}H (400 MHz), ^{13}C{^{1}H} (101 MHz), and ^{19}F NMR (377 MHz) spectra were recorded on a Bruker NMR spectrometer at room 298 K. Chemical shifts are relative to that of $SiMe_4$ (^{1}H and ^{13}C) as internal standard. ^{1}H and ^{13}C NMR assignments were made on the basis of ^{1}H-^{1}H gCOSY, ^{1}H-^{13}C gHSQC and ^{1}H-^{13}C gHMBC experiments. Elemental analysis were performed by the University of Bern Microanalytic Laboratory using a Thermo Scientific Flash 2000 CHNS-O elemental analyser. High-resolution mass spectrometry (HRMS) was carried out with a Thermo Scientific LTQ Orbitrap XL (ESI-TOF).

4.2. General procedure for the preparation of triazoles 8 and 9. A suspension of MeI (0.21 ml, 3.3 mmol) and NaN_3 (644 mg, 9.9 mmol) in H_2O/THF (14 mL; 1:1 v/v) was stirred at room temperature for 48 h. $CuSO_4.5H_2O$ (49.5 mg, 0.198 mmol), sodium ascorbate (393 mg, 1.98 mmol) and the corresponding functionalized trimethylsilyl-protected alkyne (3.96 mmol) were added subsequently and the mixture was stirred at 70 ºC for 36 h. All volatiles were removed under reduced pressure and the residue was suspended in CH_2Cl_2 (30 mL) and washed with water (2 × 50 mL), and brine (2 × 50 mL). After drying over $MgSO_4$, activated carbon was added to the solution and stirred for 30 min. The suspension was filtered through Celite, eluted

with CH_2Cl_2 (20 mL) and the filtrate was evaporated to dryness, yielding the triazole as an off-white powder.

4.3. Synthesis of 2-(1,3-dimethyl-1*H*-1,2,3λ^4-triazol-4-yl)benzo[*d*]oxazole trifluoromethanesulfonate (L1H·OTf). A suspension of 2-(1-methyl-1*H*-1,2,3-triazol-4-yl)benzo[*d*]oxazole (400 mg, 2.00 mmol) and MeOTf (249 μL, 2.20 mmol) in CH_2Cl_2 (6 mL) was stirred at –12 ºC for 20 h. Et_2O (20 mL) was added and a suspension formed. All volatiles were evaporated under reduced pressure. The residue was washed with Et_2O (3 × 10 mL) to afford **L1**H·OTf as a white solid (400 mg, 55%).

4.4. Synthesis of 2-(1,3-dimethyl-1*H*-1,2,3λ^4-triazol-4-yl)thiazole trifluoromethanesulfonate (L2H·OTf). According to the same procedure as for **L1**H·OTf from 2-(1-methyl-1*H*-1,2,3-triazol-4-yl)thiazole (597.43 mg, 3.30 mmol) and MeOTf (411 μL, 3.63 mmol) in CH_2Cl_2 (15 mL) gave a mixture of **L2**H·OTf and compound **10** in approximately 1:3 ratio (^{1}H NMR spectroscopy). Purification by column chromatography (SiO_2, CH_2Cl_2/MeOH gradient 20:1 to pure MeOH) yielded **L2**H·OTf in the first fraction (120 mg, 11%) and **10** in the second fraction (240 mg, 33%) as pale yellow waxy solids.

4.5. Synthesis of [IrCl(L1)(cod)] (1). A suspension of **L1**H·OTf (107 mg, 0.30 mmol), Me_4NCl (33 mg, 0.30 mmol), Ag_2O (140 mg, 0.6 mmol) in MeCN (8 mL) was stirred protected from light for 16 h. The suspension was then filtered through Celite, and the volatiles removed under reduced pressure. The residue was suspended in CH_2Cl_2 (8 mL) and $[Ir(cod)Cl)]_2$ (100 mg, 0.15 mmol) was added. The reaction mixture was stirred for 1 h protected from light, then filtered over Celite, and all volatiles were removed under reduced pressure. The residue was triturated with pentane, yielding product **1** as a light brown solid (90 mg, 55%). ^{1}H NMR (400 MHz, CD_2Cl_2), δ: 7.87–7.72 (m, 2H, H_{Ph}), 7.46 (m, 2H, H_{Ph}), 4.62 (bs, 1H, CH_{cod}), 4.51 (bs, 1H, CH_{cod}), 4.49 (s, 3H, NCH_3), 4.43 (s, 3H, NCH_3), 2.88 (bs, 1H, CH_{cod}), 2.80 (bs, 1H, CH_{cod}), 2.34 (bs, 1H, $CH_{2\ cod}$), 2.19 (bs, 3H, $CH_{2\ cod}$), 1.76 (bs, 2H, $CH_{2\ cod}$), 1.58 (bs, 2H, $CH_{2\ cod}$). ^{13}C{^{1}H} NMR (101 MHz, CD_2Cl_2), δ: 176.7 (C_{trz}–Ir), 154.4 (O–C=N), 150.7 (C_{Ph}), 141.7 (C_{Ph}), 133.3 (C_{trz}–C), 126.6 (C_{Ph}–H), 125.5 (C_{Ph}–H), 120.6 (C_{Ph}–H), 111.4 (C_{Ph}–H), 83.3 (CH_{cod}), 82.9 (CH_{cod}), 52.1 (CH_{cod}), 51.7 (CH_{cod}), 42.4 (NCH_3), 40.3 (NCH_3), 34.3 ($CH_{2\ cod}$), 33.7 ($CH_{2\ cod}$), 30.2 ($CH_{2\ cod}$). HRMS (ESI+): *m*/*z* found 515.1417 $[M–Cl]^+$ (calcd for $C_{19}H_{22}IrN_4O$, 515.1410). Anal. Calcd for $C_{19}H_{22}ClIrN_4O$: C, 41.49; H, 4.03; N, 10.19%. Found: C, 41.13; H,

3.87; N, 9.89%. Suitable crystals for X-ray diffraction were obtained by slow diffusion of pentane into a CH_2Cl_2 solution of **1**.

4.6. Synthesis of [IrCp*Cl(L1)]OTf (2) and [IrCp*Cl$_2$(L1)] (3). A suspension of **L1**H·OTf (107 mg, 0.30 mmol), Me_4NCl (33 mg, 0.30 mmol), Ag_2O (140 mg, 0.6 mmol) in MeCN (8 mL) was stirred protected from light for 16 h. The suspension was then filtered through Celite, and the volatiles removed under reduced pressure. The residue was suspended in CH_2Cl_2 (8 mL) and $[Ir(Cp^*)Cl_2]_2$ (90 mg, 0.11 mmol) was added. The reaction mixture was stirred for 5 h protected from light, then filtered over Celite, and all volatiles were removed under reduced pressure to yield the crude products. Purification by column chromatography (neutral Al_2O_3; CH_2Cl_2/MeCN gradient, 3:1 to pure MeCN) yielded complex **2** in the first fraction (70 mg, 32%) and complex **3** in the second fraction (25 mg, 14%) as yellow and orange solids, respectively.

[IrCp*Cl(L1)]OTf (2). ^{1}H NMR (400 MHz, CD_2Cl_2), δ: 7.86–7.78 (m, 1H, H_{Ph}), 7.77–7.70 (m, 1H, H_{Ph}), 7.66–7.56 (m, 2H, H_{Ph}), 4.58 (s, 3H, NCH_3), 4.37 (s, 3H, NCH_3), 1.92 (s, 15H, Cp–CH_3). $^{13}C\{^1H\}$ NMR (101 MHz, CD_2Cl_2), δ: 161.1 (C_{trz}–Ir), 160.4 (O–C=N), 152.0 (C_{Ph}), 137.3 (C_{Ph}), 136.3 (C_{trz}–C), 128.1 (C_{Ph}–H), 127.4 (C_{Ph}–H), 121.2 (q, $^1J_{C\text{-}F}$ = 321.27, CF_3), 117.6 (C_{Ph}–H), 113.4 (C_{Ph}–H), 91.5 (C_{Cp}), 40.6 (NCH_3), 39.3 (NCH_3), 10.4 (Cp–CH_3). ^{19}F NMR (377 MHz, CD_2Cl_2), δ: –78.92 (s). HRMS (ESI+): *m*/*z* found 577.1338 $[M–OTf]^+$ (calcd for $C_{21}H_{25}ClIrN_4O$, 577.1340). Anal. Calcd for $C_{22}H_{25}ClF_3IrN_4O_4S$: C, 36.39; H, 3.47; N, 7.72%. Found: C, 36.43; H, 3.58; N, 7.65%. Suitable crystals for X-ray diffraction were obtained by slow diffusion of pentane into a CH_2Cl_2 solution of **2**.

[IrCp*Cl$_2$(L1)] (3). ^{1}H NMR (400 MHz, $CDCl_3$), δ: 7.80–7.74 (m, 1H, H_{Ph}), 7.57–7.51 (m, 1H, H_{Ph}), 7.42–7.34 (m, 2H, H_{Ph}), 4.46 (s, 3H, NCH_3), 4.26 (s, 3H, NCH_3), 1.74 (s, 15H, Cp–CH_3). $^{13}C\{^1H\}$ NMR (101 MHz, $CDCl_3$), δ: 152.0 (C_{trz}–Ir), 151.9 (O–C=N), 149.7 (C_{Ph}), 140.4 (C_{Ph}), 135.5 (C_{trz}–C), 125.1 (C_{Ph}–H), 123.9 (C_{Ph}–H), 119.8 (C_{Ph}–H), 110.0 (C_{Ph}–H), 87.6 (C_{Cp}), 40.5 (NCH_3), 37.6 (NCH_3), 8.4 (Cp–CH_3). HRMS (ESI+): *m*/*z* found 577.1341 $[M–Cl]^+$ (calcd for $C_{21}H_{25}ClIrN_4O$, 577.1341). Anal. Calcd for $C_{21}H_{25}Cl_2IrN_4O \times H_2O$: C, 40.00; H, 4.32; N, 8.89%. Found: C, 39.51; H, 3.72; N, 8.47%. Suitable crystals for X-ray diffraction were obtained by slow diffusion of pentane into a CH_2Cl_2 solution of **3**.

4.7. Synthesis of [IrCp*Cl(L2)]OTf (4). According to the procedure described for complex 2 from **L2**H·OTf (100 mg, 0.30 mmol), Me_4NCl (33 mg, 0.30 mmol), Ag_2O (140 mg, 0.6 mmol)

in MeCN (8 mL) and[Ir(Cp*)Cl_2]$_2$ (90 mg, 0.11 mmol) in CH_2Cl_2 (8 mL) complex **4** was obtained after purification by column chromatography as a yellow solid (70 mg, 37%). ^{1}H NMR (400 MHz, $CDCl_3$), δ: 7.98 (d, $^3J_{H\text{-}H}$ = 3.5 Hz, 1H, H_{thia}), 7.75 (d, $^3J_{H\text{-}H}$ = 3.5 Hz, 1H, H_{thia}), 4.50 (s, 3H, NCH_3), 4.35 (s, 3H, NCH_3), 1.86 (s, 15H, Cp–CH_3). $^{13}C\{^1H\}$ NMR (101 MHz, $CDCl_3$), δ: 158.5 (C_{trz}–Ir), 158.3 (S–C=N), 145.7 (C_{trz}–C), 140.7 (C_{thia}–H), 122.9 (C_{thia}–H), 120.7 (q, $^1J_{C\text{-}F}$ = 320.06, CF_3), 90.8 (C_{Cp}), 39.9 (NCH_3), 38.7 (NCH_3), 9.7 (Cp–CH_3. ^{19}F NMR (377 MHz, $CDCl_3$), δ: –78.53 (s). HRMS (ESI+): *m*/*z* found 543.0961 $[M–OTf]^+$ (calcd for $C_{17}H_{23}ClIrN_4S$, 543.0950). Anal. Calcd for $C_{18}H_{23}ClF_3IrN_4O_3S_2$: C, 31.23; H, 3.35; N, 8.09; S, 9.26%. Found: C, 31.41; H, 3.00; N, 7.77; S, 9.77%. Suitable crystals for X-ray diffraction were obtained by slow diffusion of pentane into a CH_2Cl_2 solution of **4**.

4.8. Synthesis of [IrCl(L3)(cod)] (5). Compound **L3**H·BF_4 (150 mg, 0.50 mmol), Ag_2O (232 mg, 1.0 mmol) and NMe_4Cl (55 mg, 0.50 mmol) were suspended in MeCN (20 mL) and stirred for 21 h protected from light. The reaction mixture was filtered over Celite and the volatiles removed under reduced pressure. The residue was dried *in vacuo* and then suspended in dry degassed CH_2Cl_2 (15 mL). [Ir(cod)Cl]$_2$ (168 mg, 0.25 mmol) was added and the suspension stirred for 2 h protected from light under a N_2 atmosphere. The reaction mixture was filtered through Celite, and the volatiles removed under reduced pressure. Purification by column chromatography (SiO_2; CH_2Cl_2/acetone gradient 20:1 to 10:1) yielded the title product as a yellow oil which solidified upon drying thoroughly *in vacuo* and storage at –20 °C (152 mg, 55%). ^{1}H NMR (400 MHz, $CDCl_3$): δ 4.90–4.71 (m, 2H, NCH_2), 4.60–4.50 (m, 1H, CH_{cod}, 4.49–4.39 (m, 1H, CH_{cod}), 4.14 (s, 3H, NCH_3), 3.11 (s, 3H, OCH_3), 2.83–2.69 (m, 2H, CH_{cod}), 2.29–2.10 (m, 5H, $CH_{2\ cod}$ + CH_2CH_2), 2.04 (s, 3H, $C(CH_3)_2$), 2.02–1.91 (m, 1H, CH_2CH_2), 1.86 (s, 3H, $C(CH_3)_2$), 1.75–1.60 (m, 2H, CH_2CH_3), 1.58–1.40 (m, 4H, $CH_{2\ cod}$), 1.03 (t, $^3J_{HH}$ = 7.4 Hz, 3H, CH_2CH_3) $^{13}C\{^1H\}$(101 MHz, $CDCl_3$): δ 169.0 (C_{trz}–Ir), 146.7 (C_{trz}–C), 74.6 (CMe_2), 81.4 (CH_{cod}), 79.8 (CH_{cod}), 55.7 (NCH_2), 51.4 (CH_{cod}), 51.2 (OCH_3), 51.1 (CH_{cod}), 38.8 (NCH_3), 33.7 ($CH_{2\ cod}$), 33.4 ($CH_{2\ cod}$), 32.3 (NCH_2CH_2), 30.1 ($CH_{2\ cod}$), 29.6 ($CH_{2\ cod}$), 29.3 ($C(CH_3)_2$), 29.0 ($C(CH_3)_2$), 20.3 (CH_2CH_3), 13.8 (CH_2CH_3) HRMS (ESI+): *m*/*z* found 548.2008 $[M+H]^+$ (calcd. for $C_{19}H_{34}ClIrN_3O$, 548.2014) Found: 512.2243 $[M–Cl]^+$ (calcd for $C_{19}H_{33}IrN_3O$, 512.2253). Anal. Calc. for $C_{19}H_{33}ClIrN_3O$: C, 41.71; H, 6.08; N, 7.68%. Found: C, 41.71; H, 6.10; N, 7.72%. Suitable crystals for X-ray diffraction were obtained by slow diffusion of pentane into a CH_2Cl_2 solution of **5**.

4.9. Typical procedure for the transfer hydrogenation. The iridium complex (0.025 mmol) was dried under vacuum for 10 min. Under argon, ^{i}PrOH (2.5 mL), NaO^{i}Pr (0.1 M in ^{i}PrOH, 0.25 mL, 0.025 mmol) and the corresponding internal standard (0.166 mmol; mesitylene for ^{1}H NMR or dodecane for GC analysis) were sequentially added and stirred at reflux for 10 min. The reaction was initiated by adding the substrate (0.5 mmol). Aliquots were taken and were analyzed either by ^{1}H NMR spectroscopy, or by GC using the corresponding calibration curves.

4.10. Typical procedure for acceptorless oxidation of alcohols. A mixture of substrate alcohol (0.1 mmol), hexamethylbenzene (0.0165 mmol) as internal standard, and the iridium complex (0.005 mmol) in 1,2-dichlorobenzene (1.0 mL) was heated under argon at 150 ºC in a closed vial. Aliquots were taken at specified times, diluted with $CDCl_3$ and analyzed by ^{1}H NMR spectroscopy.

4.11. Crystal structure determination. Crystal data for all compounds were collected on an Oxford Diffraction SuperNova area-detector diffractometer using mirror optics monochromated Mo Kα radiation (λ = 0.71073 Å) and Al filtered. Data reduction was performed using the CrysAlisPro program.[51] The intensities were corrected for Lorentz and polarization effects, and an absorption correction based on the multi-scan method using SCALE3 ABSPACK in CrysAlisPro[51] was applied. The structure was solved by direct methods using SHELXT,[52] which revealed the positions of all nonhydrogen atoms of the title compound. The non-hydrogen atoms were refined anisotropically. All H atoms were placed in geometrically calculated positions and refined using a riding model. Refinement of the structure was carried out on F^2 using full-matrix least-squares procedures, which minimized the function $\Sigma w(Fo^2 - Fc^2)^2$. The weighting scheme was based on counting statistics and included a factor to downweight the intense reflections. All calculations were performed using the SHELXL-2014/7 program.[53] Further crystallographic details are compiled in the Supporting Information. Crystallographic data for the structures of all compounds reported in this paper have been deposited with the Cambridge Crystallographic Data Centre (CCDC) as supplementary publication numbers 1560417 (**L1**H·OTf), 1560418 (**1**), 1560415 (**2**), 1560420 (**3**), 1560419 (**4**), and 1560416 (**5**).

5. Acknowledgements

Financial support from the Spanish Ministry of Economy and Competitiveness (CTQ2016-74878-P) and European Regional Development Fund (AEI/FEDER, UE), the Catalan Government (2014SGR670), the European Research Council (CoG 615653), the Swiss National Science Foundation (R'equip 206021_128724 and 206021_170755), the Irish Research Council (Ph.D fellowship to R.P.) and the ICREA Foundation (ICREA Academia award to M.D) is gratefully acknowledged. We particularly thank COST Action CM1305 for enabling a research visit of Z.M.

We thank the group of Chemical Crystallography of the University of Bern for solving the X-ray structures of compounds **L1**H·OTf, **1**, **2** and **5** and the X-Ray Diffraction Unit of the Institut Català d'Investigació Química (ICIQ) for solving the X-ray structures of compounds **3** and **4**.

6. References

[1] a) Yoon, T. P.. Jacobsen, E. N. Privileged Chiral Catalysts. *Science*, **2003**, *299*, 1691–1693. b) Zhou, Q.-L. *Privileged Chiral Ligands and Catalysts*. Wiley-VCH: Weinheim, Germany, **2011**. c) Börner, A. *Phosphorus Ligands in Asymmetric Catalysis*; Wiley-VCH, Weinheim, **2008**.

[2] For selected reviews, see: a) Fernández-Pérez, H.; Etayo, P.; Panossian, A.; Vidal-Ferran, A. Phosphine−Phosphinite and Phosphine−Phosphite Ligands: Preparation and Applications in Asymmetric Catalysis. *Chem. Rev.* **2011**, *111*, 2119–2176. b) Guiry, P. J.; Saunders, C. P. The Development of Bidentate P,N Ligands for Asymmetric Catalysis. *Adv. Synth. Catal.* **2004**, 346, 497–537. c) Mellah, M.; Voituriez, A.; Schulz, E. Chiral Sulfur Ligands for Asymmetric Catalysis. *Chem. Rev.* **2007**, *107*, 5133–5209.

[3] For recent reviews, see: a) Diéguez, M.. Pàmies, O.; Claver, C. Ligands Derived from Carbohydrates for Asymmetric Catalysis. *Chem. Rev.* **2004**, *104*, 3189–3216. b) Diéguez, M.; Pàmies, O. Biaryl Phosphites: New Efficient Adaptative Ligands for Pd-Catalyzed Asymmetric Allylic Substitution Reactions. Acc. *Chem. Res.* **2010**, *43*, 312–322. c) van Leeuwen, P. W. N. M.; Kamer, P. C. J.; Claver, C.; Pámies, O.; Diéguez, M. Phosphite-Containing Ligands for Asymmetric Catalysis. *Chem. Rev.* **2011**, *111*, 2077–2118. d) Magre, M.; Pàmies, O.; Diéguez, M. Extending the Substrate Scope for the Asymmetric Iridium-Catalyzed Hydrogenation of Minimally Functionalized Olefins by Using Biaryl Phosphite-Based Modular Ligand Libraries. *Chem. Rec*. **2016**, *16*, 1578–1590. e) Pàmies, O.; Diéguez, M. Adaptable P-X Biaryl Phosphite/Phosphoroamidite-Containing Ligands for Asymmetric Hydrogenation and C-X Bond-Forming Reactions: Ligand Libraries with Exceptionally Wide Substrate Scope.*Chem. Rec*. **2016**, *16*, 2460–2481.

[4] a) Bourissou, D.; Guerret, O.; Gabbai, F. P.; Bertrand, G. Stable Carbenes. *Chem. Rev.* **2000**, *100*, 39–92. b) Arduengo, A. J.; Bertrand, G. Carbenes Introduction. *Chem. Rev.* **2009**, *109*, 3209–3210 (thematic issue). c) Mercs, L.; Albrecht, M. Beyond Catalysis: N-Heterocyclic Carbene Complexes as Components for Medicinal, Luminescent, and Functional Materials Applications. *Chem. Soc. Rev.* **2010**, *39*, 1903–1912. d) Herrmann, W. A. N-Heterocyclic Carbenes: a New Concept in Organometallic Catalysis. *Angew. Chem. Int. Ed.* **2002**, *41*, 1290–1309. e) Díez-González; S.; Marion, N.; Nolan, S. P. N-Heterocyclic Carbenes in Late Transition Metal Catalysis. *Chem. Rev.* **2009**, *109*, 3612–3676. f) Hahn, F. E.; Jahnke, M. C. Heterocyclic Carbenes: Synthesis and Coordination Chemistry. *Angew. Chem. Int. Ed.* **2008**, *47*, 3122–3172. g) Peris, E. Smart N-Heterocyclic Carbene Ligands in Catalysis. *Chem. Rev.*

2017, DOI: 10.1021/acs.chemrev.6b00695. (h) Glorious, F. N-Heterocyclic Carbenes in Transition Metal Catalysis, in *Topics in Organometallic Chemistry*, Springer, Berlin, 2007. i) Cazin, C. S. J. N-Heterocyclic Carbenes in Transition Metal Catalysis and Organocatalysis, Springer, Berlin, 2011. j) Díez-González, S. N-Heterocyclic Carbenes: from Laboratory Curiosities to Efficient Synthetic Tools, RSC Publishing, Cambridge, 2011. k) Huynh, H. V. *The Organometallic Chemistry of N-heterocyclic Carbenes*, Wiley, Chichester, 2017.

[5] a) Hopkinson, M. N.; Richter, C.; Schedler, M.; Glorius, F. An overview of N-heterocyclic carbenes. *Nature*, **2014**, *510*, 485–496. b) Crudden, C. M.; Allen, D. P. Stable Planar Six-π-Electron Six-Membered N-Heterocyclic Carbenes with Tunable Electronic Properties. *Coord. Chem. Rev.*, **2004**, *248*, 2247–2273. c) R. H. Crabtree, Recent Developments in the Organometallic Chemistry of N-Heterocyclic Carbenes. *Coord. Chem. Rev.*, **2007**, *251*, 595–896.

[6] For reviews, see: a) Donnelly, K. F.; Petronilho, A.; Albrecht, M. Application of 1,2,3-Triazolylidenes as Versatile NHC-type Ligands: Synthesis, Properties, and Application in Catalysis and Beyond. *Chem. Commun*. **2013**, *49*, 1145–1159. b) Crabtree, R. H. Abnormal, Mesoionic and Remote N-H heterocyclic Carbene Complexes. *Coord. Chem. Rev.* **2013**, *257*, 755–766; c) Schulze, B.; Schubert, U. S. Beyond Click Chemistry – Supramolecular Interactions of 1,2,3-Triazoles. *Chem. Soc. Rev.* **2014**, *43*, 2522–2571.

[7] Mathew, P.; Neels, A.; Albrecht, M. 1,2,3-Triazolylidenes as Versatile Abnormal Carbene Ligands for Late Transition Metals. *J. Am. Chem. Soc.* **2008**, *130*, 13534–15535.

[8] See for example: a) Aizpurua, J. M.; Fratila, R. M.; Monasterio, Z.; Perez-Esnaola, N.; Andreieff, E.; Irastorza, A.; Sagartzazu-Aizpurua, M. Triazolium Cations: from the "Click" Pool to Multipurpose Applications. *New J. Chem.* **2014**, *38*, 474–480. b) Crowley, J. D.; Lee, A.-L.; Kilpin, K. J. 1,3,4-Trisubstituted-1,2,3-Triazol-5-ylidene 'Click' Carbene Ligands: Synthesis, Catalysis and Self-Assembly. *Aust. J. Chem.* **2011**, *64*, 1118–1132. c) Schweinfurth, D.; Deibel, N.; Weisser, F.; Sarkar, B. Mit Klick zu neuen Liganden. *Nachr. Chem.* **2011**, *59*, 937–941. d) Brown, D. G.; Schauer, P. A.; Burau-Garcia, J.; Fancy, B. R.; Berlinguette, C. P. Stabilization of Ruthenium Sensitizers to TiO2 Surfaces through Cooperative Anchoring Groups. *J. Am. Chem. Soc.* **2013**, *135*, 1692–1695. e) Sinn, S.; Schulze, B.; Friebe, C.; Brown, D. G.; Jäger, M.; Kübel, J.; Dietzek, B.; Berlinguette, C. P.; Schubert, U. S. A Heteroleptic Bis(tridentate) Ruthenium(II) Platform Featuring an Anionic 1,2,3-Triazolate-Based Ligand for Application in the Dye-Sensitized Solar Cell. *Inorg. Chem.* **2014**, *53*, 1637–1645. f) Sinn, S.;

Schulze, B.; Friebe, C.; Brown, D. G.; Jäger, M.; Altuntas, E.; Kübel, J.; Guntner, O.; Berlinguette, C. P.; Dietzek, B.; Schubert, U. S. Physicochemical Analysis of Ruthenium(II) Sensitizers of 1,2,3-Triazole-Derived Mesoionic Carbene and Cyclometalating Ligands. *Inorg. Chem.* **2014**, *53*, 2083–2095. g) Guisado-Barrios, G.; Bouffard, J.; Donnadieu, B.; Bertrand, G. Crystalline 1H-1,2,3-Triazol-5-ylidenes: New Stable Mesoionic Carbenes (MICs). *Angew. Chem. Int. Ed.* **2010**, *49*, 4759–4762.

[9] For selected examples, see: a) Canseco-Gonzalez, D.; Gniewek, A.; Szulmanowicz, M.; Müller-Bunz, H.; Trzeciak, A. M.; Albrecht, M. PEPPSI-Type Palladium Complexes Containing Basic 1,2,3-Triazolylidene Ligands and Their Role in Suzuki–Miyaura Catalysis. *Chem. Eur. J.* **2012** , *18*, 6055–6062. b) Hohloch, S.; Frey, W.; Su, C.-W.; Sarkar, B. Abnormal Carbenes Derived From the 1,5-Cycloaddition Product Between Azides and Alkynes: Structural Characterization of Pd(II) Complexes and Their Catalytic Properties. *Dalton Trans.* **2013**, *42*, 11355–11358. c) Keske, E. C.; Zenkina, O. V.; Wang, R.; Crudden, C. M. Synthesis and Structure of Silver and Rhodium 1,2,3-Triazol-5-ylidene Mesoionic Carbene Complexes. *Organometallics* **2012**, *31*, 456–461. d) Keitz, B. K.; Bouffard, J.; Bertrand, G.; Grubbs, R. H. Protonolysis of a Ruthenium–Carbene Bond and Applications in Olefin Metathesis. *J. Am. Chem. Soc.* **2011**, *133*, 8498–8501. e) Lalrempuia, R.; McDaniel, N. D.; Müller-Bunz, H.; Bernhard, S.; Albrecht, M. Water Oxidation Catalyzed by Strong Carbene-Type Donor-Ligand Complexes of Iridium. *Angew. Chem. Int. Ed.* **2010**, *49*, 9765–9768. f) Prades, A.; Peris, E.; Albrecht, M. Oxidations and Oxidative Couplings Catalyzed by Triazolylidene Ruthenium Complexes. *Organometallics* **2011**, *30*, 1162–1167. h) Bolje, A.; Hohloch, S.; Urankar, D.; Pevec, A.; Gazvoda, M.; Sarkar, B.; Košmrlj, J. Exploring the Scope of Pyridyl- and Picolyl-Functionalized 1,2,3-Triazol-5-ylidenes in Bidentate Coordination to Ruthenium(II) Cymene Chloride Complexes. *Organometallics* **2014**, *33*, 2588–2598. i) Bolje, A.; Hohloch, S.; van der Meer, M.; Košmrlj, J.; Sarkar, B. Ru^{II}, Os^{II}, and Ir^{III} Complexes with Chelating Pyridyl–Mesoionic Carbene Ligands: Structural Characterization and Applications in Transfer Hydrogenation Catalysis *Chem. Eur. J.* **2015**, *21*, 6756–6764. j) Delgado-Rebollo, M.; Canseco-Gonzalez, D.; Hollering, M.; Müller-Bunz, H.; Albrecht, M. Synthesis and Catalytic Alcohol Oxidation and Ketone Transfer Hydrogenation Activity of Donor-Functionalized Mesoionic Triazolylidene Ruthenium(II) Complexes. *Dalton Trans.* **2014**, *43*, 4462–4473. k) Nakamura, T.; Terashima, T.; Ogata, K.; Fukuzawa, S. Copper(I) 1,2,3-Triazol-5-ylidene Complexes as Efficient Catalysts for Click Reactions of Azides with Alkynes. *Org. Lett.* **2011**,

13, 620–623. l) Hohloch, S.; Sarkar, B.; Nauton, L.; Cisnetti, F.; Gautier, A. Are Cu(I)-Mesoionic NHC Carbenes Associated with Nitrogen Additives the Best Cu-Carbene Catalysts for the Azide–Alkyne Click Reaction in Solution? A Case Study. *Tetrahedron Lett.* **2013**, *54*, 1808–1812. m) Heath, R.; Müller-Bunz, H.; Albrecht, M. Silver(I) NHC Mediated C–C Bond Activation of Alkyl Nitriles and Catalytic Efficiency in Oxazoline Synthesis. *Chem. Commun.* **2015**, *51*, 8699–8701.

[10] a) Meldal, M.; Tornoe, C. W. Cu-Catalyzed Azide−Alkyne Cycloaddition. *Chem. Rev.* **2008**, *108*, 2952–3015. b) Bock, V. D.; Hiemstra, H.; van Maarseveen, J. H. Cu^{I}-Catalyzed Alkyne–Azide "Click" Cycloadditions from a Mechanistic and Synthetic Perspective. *Eur. J. Org. Chem.* **2006**, 51–68. c) Worrell, B. T.; Malik, J. A.; Fokin, V. V. Direct evidence of a dinuclear copper intermediate in Cu(I)-catalyzed azide-alkyne cycloadditions. *Science* **2013**, *340*, 457–460.

[11] a) Bolje, A.; Košmrlj, J. A Selective Approach to Pyridine Appended 1,2,3-Triazolium Salts. *Org. Lett.* **2013**, *15*, 5084–5087. b) Bolje, A.; Urankar, D.; Košmrlj, J. Synthesis and NMR Analysis of 1,4-Disubstituted 1,2,3-Triazoles Tethered to Pyridine, Pyrimidine, and Pyrazine Rings. *Eur. J. Org. Chem.* **2014**, 8167–8181. c) Bolje, A.; Hohloch, S.; Košmrlj, J.; Sarkar, B. Ru^{II}, Ir^{III} and Os^{II} mesoionic carbene complexes: efficient catalysts for transfer hydrogenation of selected functionalities. *Dalton Trans.* **2016**, *45*, 15983–15993. d) Pretorius, R.; Mazloomi, Z.; Albrecht. M. Synthesis, Hemilability, and Catalytic Transfer Hydrogenation Activity of Iridium(III) and Ruthenium(II) Complexes Containing Oxygen-Functionalised Triazolylidene Ligands. *J. Organomet. Chem.* **2017**, http://dx.doi.org/10.1016/j.jorganchem.2017.05.014. e) Corbucci, I.; Petronilho, A.; Müller-Bunz, H.; Rocchigiani, L.; Albrecht, M.; Macchioni, A. Substantial Improvement of Pyridine-Carbene Iridium Water Oxidation Catalysts by a Simple Methyl-to-Octyl Substitution. *ACS Catal.* **2015**, *5*, 2714–2718. f) Petronilho, A.; Woods, J. A.; Mueller-Bunz, H.; Bernhard, S.; Albrecht, M. Iridium Complexes Containing Mesoionic C Donors: Selective $C(sp^3)$-H versus $C(sp^2)$-H Bond Activation, Reactivity Towards Acids and Bases, and Catalytic Oxidation of Silanes and Water. *Chem. Eur. J.* **2014**, *20*, 15775–15784. g) Bernet, L.; Lalrempuia, R.; Ghattas, W.; Mueller-Bunz, H.; Vigara, L. Llobet, A.; Albrecht, M. Tunable single-site ruthenium catalysts for efficient water oxidation. *Chem. Commun.*, **2011**, *47*, 8058–8060. h) Pretorius, R.; Fructos, M. R.; Müller-Bunz, H.; Gossage, R. A.; Pérez, P. J.; Albrecht, M. Synthesis and Catalytic Applications of 1,2,3-Triazolylidene Gold(I) Complexes in Silver-Free Oxazoline Syntheses and C–H Bond Activation. *Dalton Trans* **2016**, *45*, 14591–

14602. i) Woods, J. A.; Lalrempuia, R.; Petronilho, A.; McDaniel, N. D.; Müller-Bunz, H.; Albrecht, M.; Bernhard, S. Carbene Iridium Complexes for Efficient Water Oxidation: Scope and Mechanistic Insights. *Energy Environ. Sci.* **2014**, *7*, 2316–2328. j) Mendoza-Espinosa, D.; Rendón-Nava, D.; Alvarez-Hernández, A.; Angeles-Beltrán, D.; Negrón-Silva, G. E.; Suárez-Castillo, O. R. Visible-Light-Promoted Au^{I} to Au^{III} Oxidation in Triazol-5-ylidene Complexes. *Chem. Asian J.* **2017**, *12*, 203–207. k) Mendoza-Espinosa, D.; González-Olvera, R.; Negrón-Silva, G. E.; Angeles-Beltrán, D.; Suárez-Castillo, D. R.; Álvarez-Hernández, A.; Santillan, R. Phenoxy-Linked Mesoionic Triazol-5-ylidenes as Platforms for Multinuclear Transition Metal Complexes. *Organometallics* **2015**, *34*, 4529–4542. l) Modak, S.; Gangwar, K.; Rao, M. N.; Madasu, M.; Kalita, A. C.; Dorcet, V.; Shejale, M. A.; Butcher, R. J.; Ghosh, P. Fluoride-free Hiyama Coupling by Palladium Abnormal N-Heterocyclic Carbene Complexes. *Dalton Trans.* **2015**, *44*, 17617–7628. m) Saravanakumar, R.; Ramkumar, V.; Sankararaman, S. Synthesis and Structural Characterization of Cis Isomer of 1,2,3-Triazol-5-ylidene Based Palladium Complexes. *J. Organomet. Chem.* **2013**, *736*, 36–41. n) Strydom, I.; Guisado-Barrios, G.; Fernández, I.; Liles, D. C.; Peris, E.; Bexuidenhout, D. I. A Hemilabile and Cooperative N-Donor-Functionalized 1,2,3-Triazol-5-Ylidene Ligand for Alkyne Hydrothiolation Reactions. *Chem. Eur. J.* **2017**, *23*, 1393.

[12] Zamora, M. T.; Ferguson, M. J.; McDonald, R.; Cowie, M. Unsymmetrical Dicarbenes Based on N-Heterocyclic/Mesoionic Carbene Frameworks: A Stepwise Metalation Strategy for the Generation of a Dicarbene-Bridged Mixed-Metal Pd/Rh Complex. *Organometallics* **2012**, *31*, 5463–5477.

[13] For complex **2** there is some residual e-density in very close proximity to the iridium atom and the Cl atom which indicate a disorder of the metal complex about two sites. Because of the small population of the second site this disorder can't be resolved for the whole complex.

[14] Leung, C. H.; Incarvito, C. D.; Crabtree, R. H. Interplay of Linker, N-Substituent, and Counterion Effects in the Formation and Geometrical Distortion of N-Heterocyclic Biscarbene Complexes of Rhodium(I). *Organometallics* **2006**, *25*, 6099–6107.

[15] Valencia, M.; Pereira, A.; Müller-Bunz, H.; Belderrain, T. R.; Perez, P. J.; Albrecht, M. Triazolylidene-Iridium Complexes with a Pendant Pyridyl Group for Cooperative Metal–Ligand Induced Catalytic Dehydrogenation of Amines. *Chem. Eur. J.* **2017**, *23*, 8901–8911.

[16] a) Andersson, P.G; Munslow, I. *Modern Reduction Methods*; Wiley-VCH, Weinheim, **2008**. b) Gladiali, S.; Alberico, E. Asymmetric Transfer Hydrogenation: Chiral Ligands and

Applications. *Chem. Soc. Rev.* **2006**, *35*, 226–236. c) Samec, J. S. M.; Bäckvall, J.-E.; Andersson, P. G.; Brandt, P. Mechanistic Aspects of Transition Metal-Catalyzed Hydrogen Transfer Reactions. *Chem. Soc. Rev.* **2006**, *35*, 237–248. d) Wang, D.; Astruc, D. The Golden Age of Transfer Hydrogenation. *Chem. Rev.* **2015**, *115*, 6621–6686. e) Clapham, S. E.; Hadzovik, A.; Morris, R. H. Mechanisms of the H_2-Hydrogenation and Transfer Hydrogenation of Polar Bonds Catalyzed by Ruthenium Hydride Complexes. *Coord. Chem. Rev.* **2004**, *248*, 2201–2237.

[17] For selected examples, see: a) Horn, S.; Albrecht, M. Transfer Hydrogenation of Unfunctionalised Alkenes using N-Heterocyclic Carbeneruthenium Catalyst Precursors. *Chem. Commun.* **2011**, *47*, 8802–8804. b) Gnanamgari, D.; Sauer, E. L. O.; Schley, N. D.; Butler, C.; Incarvito, C. D.; Crabtree, R. H. Iridium and Ruthenium Complexes with Chelating N-Heterocyclic Carbenes: Efficient Catalysts for Transfer Hydrogenation, β-Alkylation of Alcohols, and N-Alkylation of Amines. *Organometallics* **2009**, *28*, 321–325. c) Gürbüz, N.; Özcan, E. O.; Özdemir, I.; Cetinkaya, B.; Sahin, O.; Büyükgüngör, O. Preparation of a Series of Ru(II) Complexes with N-Heterocyclic Carbene Ligands for the Catalytic Transfer Hydrogenation of Aromatic Ketones. *Dalton Trans.* **2012**, *41*, 2330–2339. d) Hillier, A. C.; Lee, H. M.; Stevens, E. D.; Nolan, S. P. Cationic Iridium Complexes Bearing Imidazol-2-ylidene Ligands as Transfer Hydrogenation Catalysts. *Organometallics* **2001**, *20*, 4246–4252.

[18] a) Maity, R.; Hohloch, S.; Su, C.-Y.; van der Meer, M.; Sarkar, B. Cyclometalated Mono- and Dinuclear Ir^{III} Complexes with "Click"-Derived Triazoles and Mesoionic Carbenes. *Chem. Eur. J.* **2014**, *20*, 9952–9961. b) Hollering, M.; Albrecht, M.; Kühn F. E. Bonding and Catalytic Application of Ruthenium N-Heterocyclic Carbene Complexes Featuring Triazole, Triazolylidene, and Imidazolylidene Ligands. *Organometallics* **2016**, *35*, 2980–2986. c) Hohloch, S.; Suntrup, L.; Sarkar, B. Arene–Ruthenium(II) and −Iridium(III) Complexes with "Click"-Based Pyridyl-triazoles, Bis-triazoles, and Chelating Abnormal Carbenes: Applications in Catalytic Transfer Hydrogenation of Nitrobenzene. *Organometallics* **2013**, *32*, 7376–7385. d) Sluijter, S. N.; Elsevier, C. J. Synthesis and Reactivity of Heteroditopic Dicarbene Rhodium(I) and Iridium(I) Complexes Bearing Chelating 1,2,3-Triazolylidene–Imidazolylidene Ligands. *Organometallics* **2014**, *33*, 6389–6397. e) Farrell, K.; Melle, P.; Gossage, R. A.; Müller-Bunz, H.; Albrecht, M. Transfer Hydrogenation with Abnormal Dicarbene Rhodium(III) Complexes Containing Ancillary and Modular Poly-pyridine Ligands. *Dalton Trans.* **2016**, *45*, 4570–4579. f) Maity, R.; Mekic, A.; van der Meer, M.; Verma, A.;

Sarkar, B. Triply Cyclometalated Trinuclear Iridium(III) and Trinuclear Palladium(II) Complexes with a Tri-Mesoionic Carbene Ligand. *Chem. Commun.* **2015**, *51*, 15106–15109.

[19] Recently, some examples of Ir-catalysts able to catalyze the TH of ketones under base-free conditions have been developed. In most of these systems, the catalyst precursor is either a metal hydride complex, or an additive is required to generate the hydride derivative in situ. See for example: a) Corberán, R.; Peris, E. An Unusual Example of Base-Free Catalyzed Reduction of C═O and C═NR Bonds by Transfer Hydrogenation and Some Useful Implications. *Organometallics*, **2008**, *27*, 1954–1958. b) Ruff, A.; Kirby, C.; Chan, B. C.; O'Connor, A. R. Base-Free Transfer Hydrogenation of Ketones Using Cp*Ir(pyridinesulfonamide)Cl Precatalysts. *Organometallics* **2016**, *35*, 327–335. c) Sepúlveda, F.; Carrión, M. C.; Phillips, A. D.; Jalón, F. A.; Dyson, P. J.; Manzano, B. R. Base-Free Transfer Hydrogenation with an Ionic-Liquid-Supported Ruthenium η^6-Arene Bis(pyrazolyl)methane Catalyst. *Eur. J. Inorg. Chem.* **2017**, 630–638. d) Bavykina, A. V.; Mautscke, H.-H.; Makkee, M.; Kapteijn, F.; Gascon, J.; Llabrés I.; Xamena, F. X. Base Free Transfer Hydrogenation Using a Covalent Triazine Framework Based Catalyst. *CrystEngComm.* **2017**, *19*, 4166–4170.

[20] Ouali, A.; Majoral, J.-P.; Caminade, A.-M.; Taillefer, M. NaOH-Promoted Hydrogen Transfer: Does NaOH or Traces of Transition Metals Catalyze the Reaction? *CatChemCat* **2009**, *1*, 504–509.

[21] For examples of related O-functionalized NHC iridium(I) complexes for efficient transfer hydrogenation catalysis, see: a) Jiménez, M. V.; Fernández-Tornos, J.; Pérez-Torrente, J. J.; Modrego, F. J.; Winterle, S.; Cunchillos, C.; Lahoz, F. J.; Oro, L. A. Iridium(I) Complexes with Hemilabile N-Heterocyclic Carbenes: Efficient and Versatile Transfer Hydrogenation Catalysts. *Organometallics* **2011**, *30*, 5493–5508. b) Jiménez, M. V.; Fernández-Tornos, J.; Pérez-Torrente, J. J.; Modrego, F. J.; García-Orduña, P.; Oro, L. A. Mechanistic Insights into Transfer Hydrogenation Catalysis by $[Ir(cod)(NHC)_2]^+$ Complexes with Functionalized N-Heterocyclic Carbene Ligands. *Organometallics*, **2015**, *34*, 926–940. c) Türkmen, H.; Pape, T.; Hahn, F. E.; Çetinkaya, B. Efficient Transfer Hydrogenation Using Iridium and Rhodium Complexes of Benzannulated N-Heterocyclic Carbenes. *Eur. J. Inorg. Chem.* **2008**, 5418–5423.

[22] For an overview of effects of O-functionalization of NHCs, see: Hameury, S.; de Frémont, P.; Braunstein, P. Metal Complexes with Oxygen-Functionalized NHC Ligands: Synthesis and Applications. *Chem. Soc. Rev.* **2017**, *46*, 632–733.

[23] The blank experiments carried out without catalyst and under different reaction conditions are shown in the Supporting Information.

[24] See for examples: a) Mestroni, G.; Zassinovich, G.; Camus, A.; Martinelli, F. Transfer of Hydrogen from Alcohols to Ketones Catalyzed by Iridium Complexes with 2,2′-Bipyridine, 1,10-Phenanthroline, and Their Derivatives. *J. Organomet. Chem.* **1980**, *198*, 87–96. b) Yang, H.; Alvarez, M.; Lugan, N.; Mathieu, R. Ruthenium(II) Complexes with New Tridentate Ligands Containing P, N, O Donor Atoms: Highly Efficient Catalysts for Transfer Hydrogenation of Ketones by Propan-2-ol. *J. Chem. Soc., Chem. Commun*. **1995**, 1721–1722. c) Dani, P.; Karlen, T.; Gossage, R. A.; Gladiali, S.; van Koten, G. Hydrogen-Transfer Catalysis with Pincer-Aryl Ruthenium(II) Complexes. *Angew. Chem. Int. Ed.* **2000**, *39*, 743–745. d) Albrecht, M.; Miecznikowski, J. R.; Samuel, A.; Faller, J. W.; Crabtree, R. H. Chelated Iridium(III) Bis-carbene Complexes as Air-Stable Catalysts for Transfer Hydrogenation. *Organometallics* **2002**, *21*, 3596–3604. e) Thoumazet, C.; Melaimi, M.; Ricard, L.; Mathey, F.; Le Floch, P. A Cationic 1-(2-Methylpyridine)Phosphole Cymene Ruthenium Chloride Complex as an Efficient Catalyst in the Transfer Hydrogenation of Ketones. *Organometallics* **2003**, *22*, 1580–1581. f) Baratta, W.; Chelucci, G.; Gladiali, S.; Siega, K.; Toniutti, M.; Zanette, M.; Zangrando, E.; Rigo, P. Ruthenium(II) Terdentate CNN Complexes: Superlative Catalysts for the Hydrogen-Transfer Reduction of Ketones by Reversible Insertion of a Carbonyl Group into the Ru-H Bond. *Angew. Chem. Int. Ed.* **2005**, *44*, 6214–6219. g) For an impressively active system with iron, see: You, W.; Lough, A. J.; Li, Y. F.; Morris, R. H. Amine(Imine)Diphosphine Iron Catalysts for Asymmetric Transfer Hydrogenation of Ketones and Imines. *Science* **2013**, *342*, 1080–1083.

[25] For successful applications in the ATH of heteroaromatic ketones, see: a) Everaere, K.; Mortreux, A.; Bulliard, M.; Brussee, J.; van der Gen, A.; Nowogrocki, G.; Carpentier, J.-F. (β-Amino Alcohol)(Arene)Ruthenium(II)-Catalyzed Asymmetric Transfer Hydrogenation of Functionalized Ketones − Scope, Isolation of the Catalytic Intermediates, and Deactivation Processes. *Eur. J. Org. Chem.* **2001**, 275–291. b) Letondor, C.; Pordea, A.; Humbert, N.; Ivanova, A.; Mazurek, S.; Novic, M.; Ward, T. R. Artificial Transfer Hydrogenases Based on the Biotin−(Strept)avidin Technology: Fine Tuning the Selectivity by Saturation Mutagenesis of the Host Protein. *J. Am. Chem. Soc.* **2006**, *128*, 8320–8328. c) Coll, M.; Pàmies, O.; Diéguez, M. Modular Hydroxyamide and Thioamide Pyranoside-Based Ligand Library from the Sugar Pool: New Class of Ligands for Asymmetric Transfer Hydrogenation of Ketones. *Adv. Synth.*

Catal. **2014**, *356*, 2293–2302. d) Matharu, D. S.; Martins, J. E. D.; Wills, M. Asymmetric Transfer Hydrogenation of C=O and C=N Bonds by Tethered Rh^{III} Catalysts. *Chem. Asian J.* **2008**, *3*, 1374–1383. e) Wu, X.; Li, X.; Zanotti-Gerosa, A.; Pettman, A.; Liu, J.; Mills, A. J.; Xiao, J. Rh^{III}- and Ir^{III}-Catalyzed Asymmetric Transfer Hydrogenation of Ketones in Water *Chem. Eur. J.* **2008**, *14*, 2209–2222. f) Baratta, W.; Chelucci, G.; Magnolia, S.; Siega, K.; Rigo, P. Highly Productive CNN Pincer Ruthenium Catalysts for the Asymmetric Reduction of Alkyl Aryl Ketones. *Chem. Eur. J.* **2009**, *15*, 726–732. g) Ito, M.; Watanabe, A.; Shibata, Y.; Ikariya, T. Synthesis and Reactivity of 2-Aminoethanethiolato-Bridged Dinuclear Ru(hmb) Complexes (hmb = η^6-hexamethylbenzene): Mechanistic Consideration on Transfer Hydrogenation with Bifunctional $[RuCl_2(hmb)]_2$/2-Aminoethanethiol Catalyst System. *Organometallics* **2010**, *29*, 4584–4592. h) Buitrago, E.; Lundberg, H.; Andersson, H.; Ryberg, P.; Adolfsson, H. High Throughput Screening of a Catalyst Library for the Asymmetric Transfer Hydrogenation of Heteroaromatic Ketones: Formal Syntheses of (*R*)-Fluoxetine and (S)-Duloxetine. *ChemCatChem* **2012**, *4*, 2082–2089. i) Margalef, J.; Slagbrand, T.; Tinnis, F.; Adolfsson, H.; Diéguez, M.; Pàmies, O. Third-Generation Amino Acid Furanoside-Based Ligands from d-Mannose for the Asymmetric Transfer Hydrogenation of Ketones: Catalysts with an Exceptionally Wide Substrate Scope. *Adv. Synth. Catal.* **2016**, *358*, 4006–4018.

[26] Farrell, K.; Müller-Bunz, H.; Albrecht, M. Synthesis, Isomerization, and Catalytic Transfer Hydrogenation Activity of Rhodium(III) Complexes Containing Both Chelating Dicarbenes and Diphosphine Ligands. *Organometallics* **2015**, *34*, 5723–5733.

[27] a) Bonomo, L; Kermovan, L.; Dupau, P. Ruthenium-Catalyzed Highly Chemoselective Hydrogenation of Aldehydes.*ChemCatChem* **2015**, *7*, 907–910. (b) Badlino, S.; Facchetti, S.; Zanotti-Gerosa, A.; Nedden, H. G.; Barratta W. Transfer Hydrogenation and Hydrogenation of Commercial-Grade Aldehydes to Primary Alcohols Catalyzed by 2-(Aminomethyl)pyridine and Pincer Benzo[h]quinoline Ruthenium Complexes. *ChemCatChem* **2016**, *8*, 2279–2288.

[28] a) Miecznikowski, J. R.; Crabtree, R. H. Transfer Hydrogenation Reduction of Ketones, Aldehydes and Imines using Chelated Iridium(III) N-Heterocyclic Bis-carbene Complexes. *Polyhedron* **2004**, *23*, 2857–2872. b) Albrecht, M.; Crabtree, R. H.; Mata, J.; Peris, E. Chelating Bis-carbene Rhodium(III) Complexes in Transfer Hydrogenation of Ketones and Imines. *Chem. Commun.* **2002**, 32–33. c) McGuinness, D. S.; Cavell, K. J.; Skelton, B. W.; White, A. H. Zerovalent Palladium and Nickel Complexes of Heterocyclic Carbenes: Oxidative Addition

of Organic Halides, Carbon−Carbon Coupling Processes, and the Heck Reaction. *Organometallics* **1999**, *18*, 1596–1605.

[29] It has been suggested that this isomerization process can proceed via the formation of Ir-π-allyl intermediates, see: ref 17a.

[30] a) Fekete, M.; Joó, F. Transfer Hydrogenation of Carbonyl Compounds and Alkenes Catalyzed by Ruthenium(II)-N-Heterocycle Carbene Complexes. *Collect. Czech. Chem. Commun.* **2007**, *72*, 1037–1045. b) Gnanamgari, D.; Moores, A.; Rajaseelan, E.; Crabtree, R. H. Transfer Hydrogenation of Imines and Alkenes and Direct Reductive Amination of Aldehydes Catalyzed by Triazole-Derived Iridium(I) Carbene Complexes. *Organometallics* **2007**, *26*, 1226–1230.

[31] These results contrast with the slow isomerization of the double bond observed using related Ru-NHC complexes, see ref. 17a.

[32] a) Pàmies, O.; Bäckvall, J.-E. Studies on the Mechanism of Metal-Catalyzed Hydrogen Transfer from Alcohols to Ketones. *Chem. Eur. J.* **2001**, *7*, 5052–5058. b) Laxmi, Y. R. S.; Bäckvall, J.-E. Mechanistic Studies on Ruthenium-Catalyzed Hydrogen Transfer Reactions. *Chem. Commun.* **2000**, 611–612.

[33] Jiménez, M. V.; Fernández-Tornos, J.; Modrego, F. J.; Pérez-Torrente, J. J.; Oro, L. A. Oxidation and β-Alkylation of Alcohols Catalysed by Iridium(I) Complexes with Functionalised N-Heterocyclic Carbene Ligands. *Chem. Eur. J.* **2015**, *21*, 17877–17889.

[34] The values of these KIE's are within the range of those obtained for other TH catalytic systems. See, for instance: a) Casey, C. P.; Singer, S. W.; Powell, D. R.; Hayashi, R. K.; Kavana, M. Hydrogen Transfer to Carbonyls and Imines from a Hydroxycyclopentadienyl Ruthenium Hydride: Evidence for Concerted Hydride and Proton Transfer. *J. Am. Chem. Soc.* **2001**, *123*, 1090–1100. b) Wettergren, J.; Buitrago, E.; Ryberg, P.; Adolfsson, H. Mechanistic Investigations into the Asymmetric Transfer Hydrogenation of Ketones Catalyzed by Pseudo-Dipeptide Ruthenium Complexes. *Chem. Eur. J.* **2009**, *15*, 5709–5718.

[35] Hansch, C.; Leo, A.; Taft, R. W. A Survey of Hammett Substituent Constants and Resonance and Field Parameters. *Chem. Rev.* **1991**, *91*, 165–195.

[36] See, for instance: a) Corey, E. J.; Suggs, J. W. Pyridinium Chlorochromate. An Efficient Reagent for Oxidation of Primary and Secondary Alcohols to Carbonyl Compounds. *Tetrahedron Lett.* **1975**, *16*, 2647–2650. b) Djerassi, C. The Oppenauer Oxidation. *Org. React.* **1951**, *6*, 207–272. c) Dess, D. B.; Martin, J. C. A Useful 12-I-5 Triacetoxyperiodinane (the

Dess-Martin Periodinane) for the Selective Oxidation of Primary or Secondary Alcohols and a Variety of Related 12-I-5 Species. *J. Am. Chem. Soc.* **1991**, *113*, 7277–7287. d) Ley, S. V.; Norman, J.; Griffith, W. P.; Marsden, S. P. Tetrapropylammonium Perruthenate, $Pr_4N^+RuO_4^-$, TPAP: A Catalytic Oxidant for Organic Synthesis. *Synthesis* **1994**, 639–666.

[37] See, for example: a) Sheldon, R. A.; Arends, I. W. C. E.; ten Brink, G. J.; Dijksman, A. Green, Catalytic Oxidations of Alcohols. *Acc. Chem. Res.* **2002**, *35*, 774–781. b) Mallat, T.; Baiker, A. Oxidation of Alcohols with Molecular Oxygen on Solid Catalysts. *Chem. Rev.* **2004**, *104*, 3037–3058. c) Piera, J.; Bäckvall, J.-E. Catalytic Oxidation of Organic Substrates by Molecular Oxygen and Hydrogen Peroxide by Multistep Electron Transfer—A Biomimetic Approach. *Angew. Chem., Int. Ed.* **2008**, *47*, 3506–3523. d) Alsafadi, D.; Paradisi, F. Effect of Organic Solvents on the Activity and Stability of Halophilic Alcohol Dehydrogenase (ADH2) from Haloferax Volcanii. *Extremophiles* **2013**, *17*, 115–122.

[38] a) Zhang, J.; Gandelman, M.; Shimon, L. J. W.; Rozenberg, H.; Milstein, D. Electron-Rich, Bulky Ruthenium PNP-Type Complexes. Acceptorless Catalytic Alcohol Dehydrogenation. *Organometallics* **2004**, 23, 4026–4033. (b) Dobereiner, E.; Crabtree, R. H. Dehydrogenation as a Substrate-Activating Strategy in Homogeneous Transition-Metal Catalysis. *Chem. Rev.* **2010**, *110*, 681–703. c) Eberle, U.; Felderhoff, M.; Schüth, F. Chemical and Physical Solutions for Hydrogen Storage. *Angew. Chem. Int. Ed.* **2009**, *48*, 6608–6630. d) Teichmann, D.; Arlt, W.; Wasserscheid, P.; Freymann, R. A Future Energy Supply Based on Liquid Organic Hydrogen Carriers (LOHC). *Energy Environ. Sci.* **2011**, *4*, 2767–2773. e) Nielsen, M.; Alberico, E.; Baumann, W.; Drexler, H.-J.; Gladiali, S.; Beller, M. Low-Temperature Aqueous-Phase Methanol Dehydrogenation to Hydrogen and Carbon Dioxide. *Nature* **2013**, *495*, 85–89.

[39] For elegant work with O-functionalized NHC iridium(III) complexes, see: a) Bartoszewicz, A.; Marcos, R.; Sahoo, S.; Inge, A. K.; Zou, X.; Martín-Matute, B. A Highly Active Bifunctional Iridium Complex with an Alcohol/Alkoxide-Tethered N-Heterocyclic Carbene for Alkylation of Amines with Alcohols. *Chem. Eur. J.* **2012**, *18*, 14510–14519. b) Bartoszewicz, A.; González Miera, G.; Marcos, R.; Norrby, P.-O.; Martín-Matute, B. Mechanistic Studies on the Alkylation of Amines with Alcohols Catalyzed by a Bifunctional Iridium Complex. *ACS Catal.* **2015**, *5*, 3704−3716. c) González Miera, G.; Martínez-Castro, E.; Martín-Matute, B. Acceptorless Alcohol Dehydrogenation: OH vs NH Effect in Bifunctional NHC–Ir(III) Complexes. *Organometallics* **2017** (doi 10.1021/acs.organomet.7b00220).

[40] a) Canseco-Gonzalez, D.; Albrecht, M. Wingtip Substituents Tailor the Catalytic Activity of Ruthenium Triazolylidene Complexes in Base-free Alcohol Oxidation. *Dalton Trans.* **2013**, *42*, 7424–7432. b) Bagh, B.; McKinty, A. M.; Lough, A.J.; Stephan, D. W. 1,2,3-Triazolylidene Ruthenium(II)(η^6-arene) Complexes: Synthesis, Metallation and Reactivity. *Dalton Trans.* **2014**, *43*, 12842–12850. c) Van der Meer, M.; Glais, E.; Siewert, I.; Sarkar, B. Electrocatalytic Dihydrogen Production with a Robust Mesoionic Pyridylcarbene Cobalt Catalyst. *Angew. Chem. Int. Ed.* **2015**, *54*, 13792–13795.

[41] Gunanathan, C.; Shimon, L. J.; Milstein D. Direct Conversion of Alcohols to Acetals and H2 Catalyzed by an Acridine-Based Ruthenium Pincer Complex. *J. Am. Chem. Soc.* **2009**, *131* 3146–3147.

[42] Valencia, M.; Müller-Bunz, H.; Gossage, R. A.; Albrecht, M. Enhanced Product Selectivity Promoted by Remote Metal Coordination in Acceptor-free Alcohol Dehydrogenation Catalysis. *Chem. Commun.* **2016**, *52*, 3344–3347.

[43] The difference in the rate determining step of transfer hydrogenation and in the base-free dehydrogenation reactions can be rationalized by the absence of base in the later process. The presence of base is key in the formation of the hydride as active species in the transfer hydrogenation. In the absence of base, such alkoxides cannot form easily and instead, a solvolysis takes place for the alcohol substrate to coordinate to the metal center.

[44] a) Aslanian, R. G. Patent WO2012051036, 2012. b) Geronikaki1, A.; Vasilevsky, S.; Hadjipavlou-Litina1, D.; Lagunin, A.; Poroikov, B. V. Synthesis and Anti-inflammatory Activity of Ethynylthiazoles. *Chemistry of Heterocyclic Compounds*, **2006**, *42*, 675–680.

[45] Khasanov, A. B.; Ramirez-Weinhouse, M. M.; Webb,Th. R.; Thiruvazhi, M. Novel Asymmetric Approach to Proline-Derived Spiro-β-lactams. *J. Org. Chem.* **2004**, *69*, 5766–5769.

[46] Slagbrand, T.; Lunderg, H.; Adolfsson, H. Ruthenium-Catalyzed Tandem-Isomerization/Asymmetric Transfer Hydrogenation of Allylic Alcohols. *Chem. Eur. J.* **2014**, *20*, 16102–16106.

[47] Limmert, M. E.; Roy, A. H.; Hartwig, J. F. Kumada Coupling of Aryl and Vinyl Tosylates under Mild Conditions *J. Org. Chem.* **2005**, *70*, 9364–9370.

[48] Baciocchi, E.; Ruzziconi, R. Electronic and Steric Effects in the Addition of Electrophilic 1,3-Dicarbonylalkyl Radicals to Styrenes. *J. Org. Chem.* **1991**, *56*, 4772–4778.

[49] Barton, D. H. R.; Bohe, L.; Lusinchi, X. The Action of Sodium Hydrogen Telluride on Olefins. *Tetrahedron*, **1990**, *46*, 5273–5284.

[50] Casey, Ch. P.; Johnson, J. B. Kinetic Isotope Effect Evidence for a Concerted Hydrogen Transfer Mechanism in Transfer Hydrogenations Catalyzed by [p-(Me_2CH)C_6H_4Me]Ru-(NHCHPhCHPhN$SO_2C_6H_4$-p-CH_3). *J. Org. Chem.* **2003**, *68*, 1998–2001.

[51] Oxford Diffraction (2010). CrysAlisPro (Version 1.171.34.44). Oxford Diffraction Ltd., Yarnton, Oxfordshire, UK.

[52] Sheldrick, G. M. SHELXT – Integrated Space-Group and Crystal-Structure Determination. *Acta Cryst.* **2015**, *A71*, 3–8.

[53] Sheldrick, G. M. Crystal Structure Refinement with SHELXL. *Acta Cryst.* **2015**, *C71*, 3–8.

For Table of Contents Only

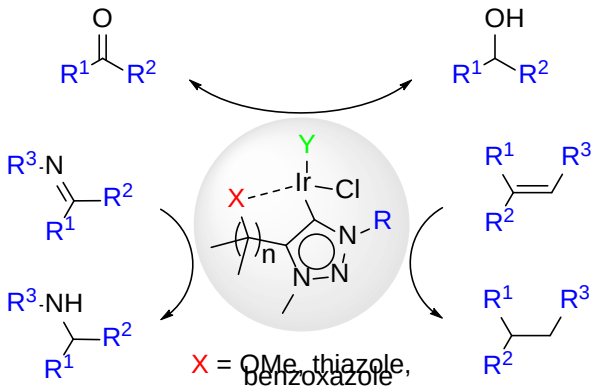

New triazolylidene iridium containing complexes for highly efficient and versatile transfer hydrogenation of C=O, C=N and C=C bonds, and for alcohol dehydrogenation are reported. A set of mechanistic studies have identified distinct rate determining steps for transfer hydrogenation and for acceptorless alcohol oxidation. These results underline the relevance of ligand design principles, and they provide guidelines for further optimization and for the design of new efficient systems.